

**Fast Train Track Quality Measurement Using Gyro  
Sensors**

By

Muhamad Nizam Bin Mustapha

15895

Dissertation submitted in partial fulfilment of  
the requirements for the  
Bachelor of Engineering (Hons)  
(Electrical & Electronics Engineering)

JAN 2016

Universiti Teknologi PETRONAS

Bandar Seri Iskandar

31750 Tronoh

# CERTIFICATION OF APPROVAL

## **Fast Train Track Quality Measurement Using Gyro Sensors**

By

Muhamad Nizam Bin Mustapha

15895

A project dissertation submitted to the

Electrical & Electronics Engineering Programme

Universiti Teknologi PETRONAS

in partial fulfillment of the requirement for the

BACHELOR OF ENGINEERING (Hons)

(ELECTRICAL AND ELECTRONICS)

Approved by,

---

(Dr Fawnizu Azmadi B Hussin)

UNIVERSITI TEKNOLOGI PETRONAS

TRONOH, PERAK

JAN 2016

## CERTIFICATION OF ORIGINALITY

This is to certify that I am responsible for the work submitted in this project, that the original work is my own except as specified in the references and acknowledgements, and that the original work contained herein have not been undertaken or done by unspecified sources or persons.

---

MUHAMAD NIZAM MUSTAPHA

## ABSTRACT

A proposed project entitled “Fast Train Track Quality Measurement Using Gyro Sensors” has been conducted for vibration detection system on railway track. This paper is to describe the collection of vibration data on a train coach to see patterns of abnormalities along the way from Batu Gajah station to KL Sentral station. Focusing on designing a portable vibration system that can detect the deformation of railway track with good accuracy of accelerometers, and gyro sensors. Data collected from the system was analyzed where abnormalities are identified and compare relative to location of railway track. While the Direct-Cosine-Matrix (DCM) was applied to get the raw data from the Inertia Measurement Unit (IMU) sensor for both acceleration and tilt movement of the train. Using MATLAB, data processing will be take part in converting the data into graphs for differentiating the vibration noise and real data. To reduce the high frequency vibration from the train itself, low pass filter (Finite Impulse Response) will be program along the data processing to get better visualization of the vibration itself. Throughout the testing, few locations has been identified for abnormalities of the vibration movement from Rawang to Kuala Lumpur Station. Due to this abnormal vibrations, the comfort level in passenger is low as compared the final testing of the system.

## **ACKNOWLEDGMENT**

First and foremost, I would like to praise and thankful to Allah SWT for giving me strengthens in obtains a successful report Final Year Project titled “Fast Train Track Quality Measurement Using Gyro Sensors”. My utmost gratitude to my beloved Supervisor, Dr Fawnizu Azmadi Hussin and co-Supervisor, Dr Abu Bakar Sayuti for all their kindness and supportive moments on me along finishing this project report. Their full commitment in supervising and giving motivation such a huge impact on me. Not to forget to all members and course-mate from Electrical and Electronic Engineering Department for all the efforts and ideas directly or indirectly to make sure this project had its best and success. Then, special thanks to my parent, Mustapha Bin Sidin, and Noorizan Binti Mohamed for all their support at the beginning of my career as engineering students starting 2011 until now. Lastly, I would like to thanks from Management Unit in Universiti Sains Malaysia (USM), Penang for giving me opportunity to survey their equipment for lab testing, also not to forget, person in charge from Universiti Tun Hussein Onn Malaysia (UTHM), Batu Pahat for taking for lab survey in UTHM. Without all the supports, I believe it would be hard for me to achieve what I have now.

## TABLE OF CONTENTS

<b>CERTIFICATION OF APPROVAL</b>	.	.	.	.	<b>i</b>
<b>CERTIFICATION OF ORIGINALITY</b>	.	.	.	.	<b>ii</b>
<b>ABSTRACT</b>	.	.	.	.	<b>iii</b>
<b>ACKNOWLEDGMENT</b>	.	.	.	.	<b>iv</b>
<b>CHAPTER 1: INTRODUCTION.</b>	.	.	.	.	<b>1</b>
1.1	Background of Study	.	.	.	1
1.2	Problem Statement	.	.	.	2
1.3	Objectives	.	.	.	2
1.4	Scope Study	.	.	.	2
<b>CHAPTER 2: LITERATURE REVIEW</b>	.	.	.	.	<b>3</b>
2.0	Introduction	.	.	.	3
2.1	General Information on Train's Transportation	.	.	.	3
2.1.1	KTMB Intercity Passenger Rail	.	.	.	3
2.1.2	Intercity Commuter Rail)	.	.	.	4
2.2	Railway Track in Malaysia	.	.	.	5
2.2.1	Superstructure and Substructure	.	.	.	5
2.2.2	Rail	.	.	.	6
2.3	Type of Detection System	.	.	.	7
2.3.1	Neuro-Fuzzy System	.	.	.	7
2.3.2	Position Sensitive Device method	.	.	.	8
2.4	Hardware Study	.	.	.	8
<b>CHAPTER 3: METHODOLOGY</b>	.	.	.	.	<b>10</b>
3.0	Introduction	.	.	.	10
3.1	Project Activities	.	.	.	10
3.2	Project Milestones	.	.	.	10
3.2.1	First Phase	.	.	.	11
3.2.2	Second Phase	.	.	.	11
3.3	Hardware Setup	.	.	.	13
3.4	Data Post Processing	.	.	.	14
3.5	Hardware-Software Interface	.	.	.	15
3.6	Direct Cosine Matrix (DCm) Algorithm	.	.	.	15
<b>CHAPTER 4: RESULT</b>	.	.	.	.	<b>19</b>
4.0	Output Data	.	.	.	21
4.1	Lab Testing	.	.	.	21
4.1.1	Equipment Setup	.	.	.	21
4.1.2	Data Collection	.	.	.	23
4.2	Car-Mounted Field Testing	.	.	.	30
4.3	Train-Mounted Field Testing	.	.	.	34
4.3.1	Overall Measurement System	.	.	.	37

4.3.2 Track Characteristics	39
<b>CHAPTER 5: CONCLUSION AND RECOMMENDATION</b>	<b>42</b>
<b>REFERENCES:</b>	<b>43</b>
<b>APPENDIX</b>	<b>45</b>

## LIST OF FIGURES

FIGURE 1. Keretapi Tanah Melayu Berhad (KTMB) railway tracks [8].....	4
FIGURE 2. LRT trains used in Malaysia [9] .....	5
FIGURE 3. Typical ballasted track profile [12].....	6
FIGURE 4. Ultrasonic Transducers Arrangement [15].....	8
FIGURE 5. Inertia Measurement Unit .....	10
FIGURE 6. Interface ArduIMU with USB-UART Converter .....	13
FIGURE 7. Example of Output (Graph) .....	14
FIGURE 8. Direct Cosine Matrix (DCM) Algorithm Block Diagram.....	15
FIGURE 9. Program flowchart representing the workflow of interfacing between PC and IMU.....	18
FIGURE 10. Output Data on Serial Monitor.....	19
FIGURE 11. Output Data in Text File (.txt) .....	20
FIGURE 12. Output Data in Excel File (.xls) .....	20
FIGURE 13. Vibration Shaker .....	21
FIGURE 14. Prototype Platform .....	21
FIGURE 15. Z Axis Interface .....	22
FIGURE 16. Y Axis Interface .....	22
FIGURE 17 X Axis Interface .....	22
FIGURE 18. Software Interface 20 Hz .....	23
FIGURE 19. z Orientation ( 1G ) .....	24
FIGURE 20. y Orientation ( 1G ).....	24
FIGURE 21. x Orientation ( 1G ).....	25
FIGURE 22. z Orientation ( 1G ).....	25
FIGURE 23. y Orientation ( 1G ).....	26
FIGURE 24. x Orientation ( 1G ).....	26
FIGURE 25. z Orientation ( 1.5G ).....	27
FIGURE 26. y Orientation ( 1.5G ).....	27
FIGURE 27. x Orientation ( 1.5G ).....	27
FIGURE 28. z Orientation ( 0.1G ).....	28
FIGURE 29. y Orientation ( 0.1G ).....	28
FIGURE 30. x Orientation ( 0.1G ).....	29



FIGURE 31. 0Hz Frequency .....	29
FIGURE 33. Car-Mounted Field Testing hump.....	30
FIGURE 32. Axis Position .....	30
FIGURE 34. Collected IMU data for car-mounted field testing over distance.....	32
FIGURE 35. Close-up on pitch angle, x-axis acceleration and z-axis acceleration as car passes through second bump. ....	33
FIGURE 36. Collected IMU data for car-mounted field testing over distance (FIR) .....	34
FIGURE 37. KTM Stations from Batu Gajah to Kuala Lumpur .....	35
FIGURE 38. Collected IMU data for train-mounted field testing, covering from Kampar Station to KL Sentral Station.....	36
FIGURE 39. Axis Position .....	37
FIGURE 40. Distance coverage for train-mounted field testing.....	38
FIGURE 41. z axis acceleration measurement in KM178.6 to KM179.3.....	39
FIGURE 42. y axis acceleration between KM142.5 to KM145.5.....	40
FIGURE 43. Vertical acceleration measurement in KM181.25 to KM186.5. ....	40
FIGURE 44. Roll angle measurement in KM132 to KM135.5.....	41

## **LIST OF TABLES**

Table 1. Malaysia’s Electrified Double Track Project .....	1
Table 2. Types of rail profiles and their applications [12] .....	6
Table 3. Gantt chart .....	12
Table 4. Connection Pin Interfacing USB-UART and IMU .....	14
Table 5. Approximately distance for each station .....	37

# CHAPTER 1

## INTRODUCTION

### 1.0 INTRODUCTION

This report will discuss the overall overview of the progress of a Final Year Project (FYP1 & FYP2). It will be covering the studies on the viability of using a set of low cost motion sensors (IMU) in order to identify any possibility misalignments in a railway track. The project is a continuation of ideas in order to come out motion design with low cost of implementation that can easily applied in any transportation to get the x,y,z axis for both acceleration and movements.

### 1.1 Background Statement

The Malaysian railways can be classified as a dynamic entity that has the opportunity to gain their important achievements in order to develop a sustainable transportation system in the country. They're facing the obstacles to improve their consistency and rapidity in order to gain competitive services and become one of the successful road alternative [1]. There's a lot of innovation has been made for improvement on train's transportation. Railway tracks was developed with same characteristics, as for now includes common railway, electrified railway, high-speed rail, and monorail [21].

Around 179 km of the main West Coast line has the double-tracking project that enables Kereta Api Tanah Melayu Berhad (KTMB) to provide trains at a maximum speed of 160 km/h from Seremban via KL Sentral to Ipoh. Table 1 shows the difference between the track system from Padang Besar-Ipoh and Seremban-Gemas [3], [4].

Table 1. Malaysia's Electrified Double Track Project

Ipoh- Padang Besar	Seremban-Gemas
329km long with 15 stations, 8 halts, and 2 tunnels.	98km long with 6 stations
Scheduled to be completed by 7 November 2014. As of July 2012, the overall progress of the project is 86.72%.	Scheduled to be completed by 31 July 2013. As of July 2012, the overall progress of the project is 90.55%.
Equipped with modern signaling, communication and electrification system.	

## **1.2 Problem Statement**

Many systems are in use on the world's railroads. These devices apply infrared and laser scanning technologies, and even ultrasonic audio analysis. These systems have been used over 70 years and are currently still in use on worldwide railway tracks. In Malaysia, railway tracks have been updated with modern signaling, and electrification railway systems. For this project, a framework should be made with sensors that can recognize both horizontal and vertical deviations to identify signs of misalignment and low nature of the track.

## **1.3 Objectives of Study**

Main objective of this project is;

- i. To design and develop a portable hardware-software system that can record data related to movement and vibration in a train.
- ii. To analyze recorded data so that locations where possible track-misalignment are present can be identified.

## **1.4 Scope of Study**

This project focuses on two tasks, i.e. recording of data related to motion inside a train coach, and secondly analysis of the data to identify patterns that correlate to track irregularities. This involves designing a motion and vibration detection hardware-software system, interfacing of sensors, microcontroller and a personal computer, and data processing using MATLAB software.

## **CHAPTER 2.0**

### **LITERATURE REVIEW**

#### **2.0 Introduction**

In this chapter, previous researches and studies that are related to the project will be discussed. The literatures will be divided into parts which are general information regarding train's transportation in Malaysia, previous technologies that has been explored to detect misalignment railway and hardware study.

#### **2.1 General Information on Train's Transportation in Malaysia**

Unpredictable traffic conditions in Malaysia have led into alternative public transport for travelling the urbanities. To overcome this issue, railway industries has been come out a few elements (e.g. Manpower development, rails infrastructure and rail technology) to ensure rail activities can reach its progressive level [5]. Early 1885, first railway track was built from Taiping to Port Weld (13 kilometers). Then followed by short railway tracks in order to connect mining areas to ports starting from West Coast of Peninsular Malaysia. By the late 20<sup>th</sup> century, both northern and southern areas of the Peninsular Malaysia were connected to give more advance on its industries [6].

Malaysia has 2418KM of total track which 57KM use Standard (1.435 M) gauge and 2361KM use Narrow (1.000M) gauge. Approximately 150 KM of rail in Malaysia is electrified. Malaysia had a largest railroad which known as Keretapi Tanah Melayu Berhad (KTMB); originally named as Malayan Railway, and owned 2262 KM out of 2418 KM of tracks in Malaysia. While the remaining of it was stated for Sabah State Railway. KTMB has been divided into two (2) operations which is KTMB Intercity Passenger Rail and Intercity Commuter Rail [1].

##### **2.1.1 KTMB Intercity Passenger Rail**

Heavy rail basically used for intercity passenger and freight transport, together used for some urbanistic transportation [5]. Currently there already 24 intercity passengers trains has been runs daily, consist of 16 express trains and 8 local trains [7]. This service has it's prioritize in Malaysia due to the increasing of mobility of people. Figure 1 shows the railway tracks for KTMB intercity railway trains consists of North-South Line (Butterworth-Woodlands) and East-South Line (Tumpat-

Woodlands). Intercity trains has an average speed around 50 km/h, and this can results in delay of services when it operates during peak hours or season duration. Frequent delay has cause KTMB some problems that can lead into substantial nuisance to the passengers and reduces the utility of the system [8].

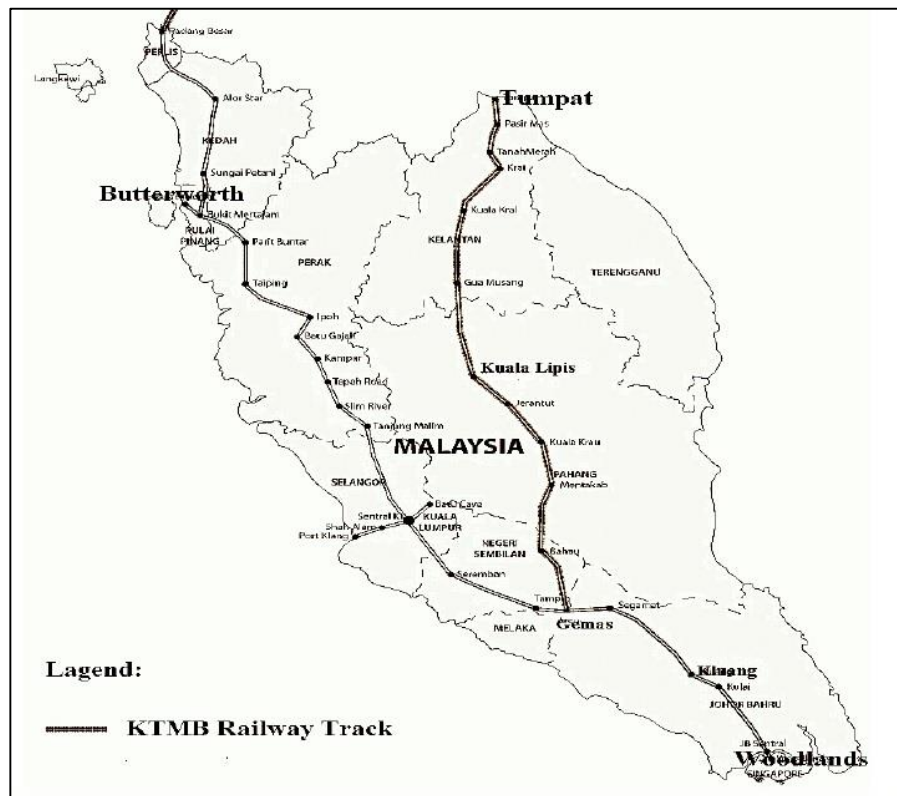


FIGURE 1. Keretapi Tanah Melayu Berhad (KTMB) railway tracks [8]

### 2.1.2 Intercity Commuter Rail

Availability of Commuter Rail and Light Rail Transit (LRT) in Kuala Lumpur are probably used for urban public transport. Interconnection points between LRT and Commuter Rail between Sentral Kuala Lumpur including Bank Negara and Bandar Tasik Selatan. Interconnections between Sentral Kuala Lumpur with Kuala Lumpur International Airport (KLIA) by using high-speed rail line with two high-speed train services [1], [5]. In 2003, it has been reportedly that Commuter Rail could handles approximately 70000 passengers per day. KTM Komuter provides 40 stations with 213 trains runs daily from Monday through Friday, 218 trains on Saturdays and 177 trains on Sundays [1]. LRT systems in Kuala Lumpur area divided into two systems; STAR (Sistem Transit Aliran Ringan) and PUTRA (Projek Usahasama Transit Ringan Automatik). PUTRA is an electrically-powered trains operates on double tracks, fully automated, and driverless system. While STAR system is a driver-

operated system, partially elevated and at-grade. Figure 2 shows LRT trains used by KTMB Malaysia [9].



FIGURE 2. LRT trains used in Malaysia [9]

## 2.2 Railway Track in Malaysia

Increase in demanding better system consistency, availability, maintainability, and safety railway track for public usage become the most important studies in railway industry [10]. The Malaysian railroads are in fact a dynamic, assorted corporatized substance that can possibly play important part in the improvement of a practical transportation framework in the nation. Indeed, in order to be competitive and enhance their importance as another alternative in Malaysian roads, the system must be able to face any challenges to improve their reliability and speed [1].

The ability of modern railway systems was capable enough to drive fast trains and large loads. Structural integrity of the soil must be the primary requirement because it determines the suitability of steel for rail track applications. It depends on connections between engineering parameters, material properties and the environment. To prevent any failure, the track material must be a high standard of straightness and flatness [11].

### 2.2.1 Superstructure and Substructure

Fundamental part of railway infrastructure and its components can be classified into two parts, superstructure and substructure. Superstructure probably referred as rails, rail pads, concrete sleepers, and fastening systems while substructure is related with a geotechnical system which is ballast, sub-ballast and subgrade. Both structure are basically important in preventing any failure and to ensure passengers' safety [12].

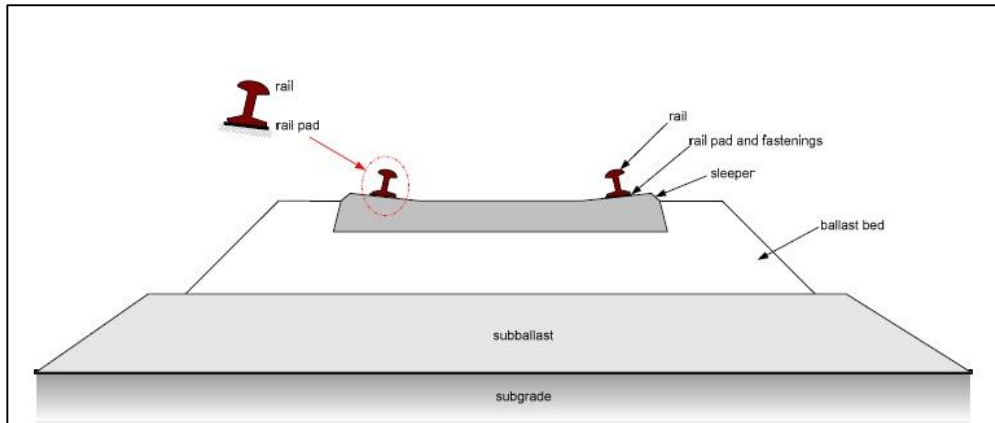
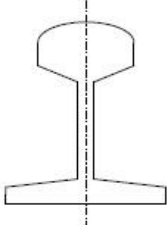
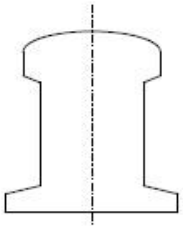
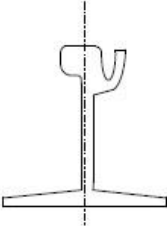


FIGURE 3. Typical ballasted track profile [12]

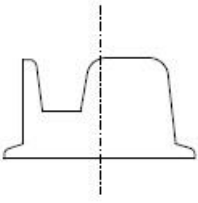
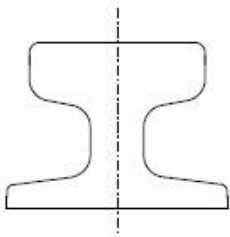
### 2.2.2 Rail

Rail is the track longitudinal steel element which is placed on spaced sleepers to guide the rolling stock. It must be sufficient enough to maintain a steady shape and smooth track configuration, and sustain the loads applied in vertical, longitudinal, and lateral directions. This could ensure the proper functioning of rails in the track system [12], [13]. Table 2 shows the types of rail used in railway tracks and their applications.

Table 2. Types of rail profiles and their applications [12]

Shape	Profile Type	Applications
	Flat-bottom rail	Standard rail track
	Construction rail	Manufacturing of automobiles and switch parts
	Grooved rail	Railway track embedded in pavements, roads, yards



	<p>Block rail</p>	<p>Railway track used in concrete slab as part of Nikex-structure</p>
	<p>Crane rail</p>	<p>Heavy load hoisting cranes with high wheel loads</p>

### 2.3 Detection Methods

Different types of system have been applied to create vibration detection system. These various systems are available so that the system can always be compatible along with the modernization and be kept updated with the best accuracy. Compatibility and sustainability of the systems in detecting any misalignment also will be count in order to differentiate better accuracy of the tracks.

#### 2.3.1 Neuro – Fuzzy System

Neuro-Fuzzy system is the combination of both Fuzzy Logic and Neural Networks, unified from hybrid adaptive networks [14]. Since its ability to identify irregularities of pattern created in the data, then it was determine to improve the automated detection and ordering of rail failure. The system will be mounted ultrasonic transducers at the wheels to collect data from the rail. These transducers located at the Figure 4 below. The result must be consistently on data taken from different types and ages of rails, and from different locations [15].

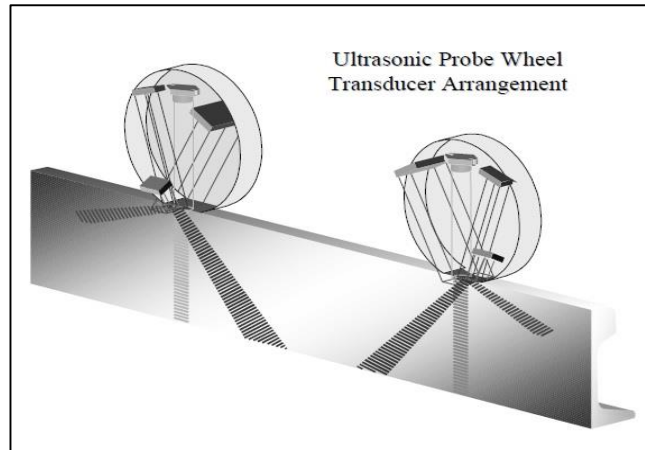


FIGURE 4. Ultrasonic Transducers Arrangement [15]

Adaptive network-fuzzy inference system (ANFIS) could improve system performance in detecting misalignments. FIS was embedded into neural networks, which allows the use of fuzzy rules in use of testing data to improve system performance. In any case, an ANFIS is a single-output classification model, which resulting poor accuracy in input-output mapping data [16].

### 2.3.2 Position Sensitive Device (PSD) method

Flat wheels of the train may be one of the possibility of vibration movement of the train itself, due to the impact created between wheels and rail collision [17]. This system actually has been used in different target position determining apparatus, due to its easy way of installation and high speed operation. PSD is a semiconductor device and consists of resistance layer, photosensitive layer and bias layer [18]. This method can detect the flat wheels while the train passed by using the variance value of frequencies of demodulated light sources [17], [19]. Also known as Optoelectronic device, it is easy to set up and it is suitable for detecting the impacts on railway tracks as PSD is sensitive to the barycenter of light spot illuminated simultaneously on the track surface [20].

### 2.4 Hardware Study

Choosing a good hardware that compatible with other components is the first criteria need to be applied in doing any system. USB to UART Converter (UC00A) will be connected to ArduIMU V3 to gain data from the sensor itself. UART is an interface serial communication between devices and applies to microcontroller and computer.

Back to history, serial interface between microcontrollers to computer is through serial port (DB9) [21].

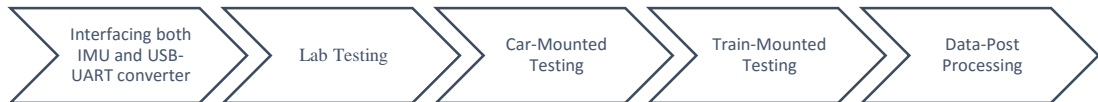
ArduIMU+ V3 is an Inertial Measure Unit (IMU), and on-board Arduino compatible processor by combining new Invensense MPU-6000 MEMS 3-axis gyro and accelerometer, and 3-axis I2C magnetometer (HMC-5883L) [22]. Even ArduIMU+ V3 is a tiny compare to Version 2 and Version 1, but with combination of GPS port and on-board Atmega328 microprocessor, this version yet powerful in Six Degree of Freedom orientation performances. This version is a breadboard friendly, and this advantage can lead into its suitability for any application in any movement detection [23].

## CHAPTER 3

### METHODOLOGY

#### 3.0 INTRODUCTION

In this chapter, further elaboration will be discussed in order to achieve the objectives through project activities and method. As the flow of the project was divided into five (5) phases as described below.



#### 3.1 Project Activities

An ArduIMU+ V3 acted as the main component of the prototype. Version 3 has been improved by incorporating MPU-6000 MEMS based accelerometer and gyroscope sensor, thus it supports a complete set of information on the degree of freedom (DOF) in movement, acceleration and tilt. MPU-6000 uses SPI (Serial Peripheral Interface) instead of I2C for max performance.

As shown in Figure 5, gyroscope sensor is capable of measuring tri-axis, yaw, pitch, and roll orientation, while accelerometer sensor manages to detect both static and dynamic acceleration, mainly used to detect acceleration with respect to x, y, and z axis.

USB-to-UART converter will be connected through ArduIMU+ to give instruction, send data from IMU into the computer system.

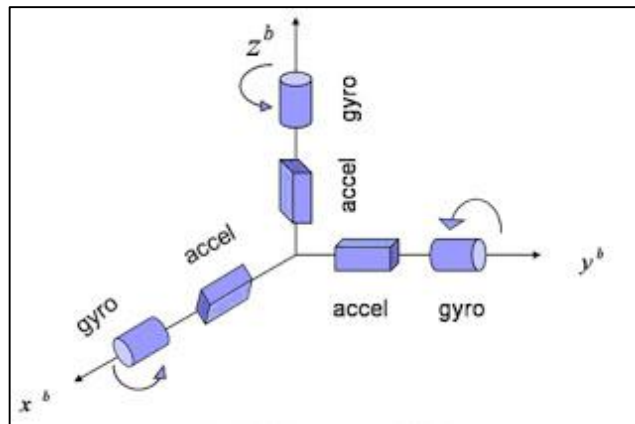


FIGURE 5. Inertia Measurement Unit

## **3.2 Project Milestones**

Key milestones of this project will be divided into two phases, which will be cover in this point

### **3.2.1 First Phase**

#### **ArduIMU+ V3 Sensor and USB-to-UART Converter Interface**

First of all, the ArduIMU+ V3 sensor must be successfully integrated with a USB-to-UART converter (UC00A). The converter basically offers USB plug and play, which can directly interface with microcontroller with low current 5 V supply from the USB port. The reasons of using UC00A to interface the IMU sensor because it's easy to use in aiming development between computer and microcontroller, 5V logic. Plus its compatibility for Window XP and Vista and it appear as a Virtual COM port on computer. Once the integration is success, few tests must be done inability to read data of six degrees of freedom which is tri-axis acceleration, together with tri-Euler movement.

#### **Record and Store IMU data**

In this part, all the data will be transferred into PC system through USB-to-UART converter. The data collected will be saved in excel file format (csv). The data will be divided into six (6) columns which is tri-axis accelerations, and tri-Euler movement. Data collected will be directly filtered through the code itself as we will reprogram the IMU sensors together with DCM algorithm.

### **3.2.2 Second Phase**

#### **Visualization Data**

Recorded data will be visualized through MATLAB and it will convert into graphical. The data already filtered by using DCM algorithm. Direction Cosine Matrix (DCM) algorithm is the next step in stabilization and control function of any movement. This is important due the data collected is not coming from the train itself, but the system also read some noise coming from different angle of the train. We need to analyses possible noise are coming from the trains itself, the mass of the train, including the total mass if the coach in full passenger.

Table 3. Gantt chart

Main Task	First Semester/ Week														Second Semester/ Week														
	1	2	3	4	5	6	7	8	9	10	11	12	13	14	1	2	3	4	5	6	7	8	9	10	11	12	13	14	
Literature Review	■																												
Identify suitable hardware and purchasing				■																									
Extended Proposal						★																							
Assembly and initial testing							■																						
Proposal Defense							★	★																					
Hardware setup and testing							■																						
Programming through Arduino IDE								■																					
Prototype calibration & experimental testing														■															
Interim Report													★	★															
Data collection												■								■									
Progress Report																					★								
Data processing																					■								
Project Dissertation and Presentation																											★	★	★

## Data Analysis Interpretation

Converted data will be analysed so that output can be estimated as the final result. Few tests need to be done so that the few results can be analysed for comparisons in order to get predictable results. Lab testing will be conducted to analyze typical movement of the both acceleration, and gyroscope so that there will be comparison to see any changes of vibration movement in railway tracks later on.

### 3.3 Hardware Setup

Six degrees of freedom (DOF) accelerometer and gyroscope IMU sensor will be used as a motion sensor to detect any irregularities at railway track. ArduIMU+ V3 which is furnished with MPU-6000 MEMS-based tri-axis gyros and tri-axis accelerometer, I2C Magnetometer (HMC-5883L) and Arduino ATmega328 microcontroller running 16 MHz has been purchased for this project.

In addition, GPS will be optionally added into the system to give accuracy on the location detected for any misalignment on the track. IMU sensor will be connected directly to USB-to-UART converter to read the serial communication between both PC system and microcontroller.

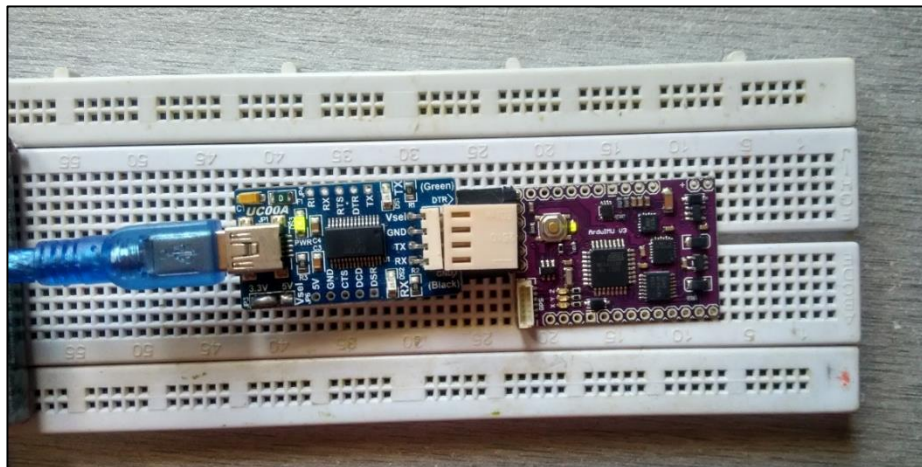


FIGURE 6. Interface ArduIMU with USB-UART Converter

Both IMU and USB-UART converter need to be soldered with 6-pins header socket before interfacing both components. The 'Vsel' pin of USB-UART converter will be connected through soldering with 3.3V jumper to the middle pad and so that it could supply the rated voltage as the input to the IMU, where the Arduino Atmega328 could

support input voltage from 1.8V to 5.5V. The connection table for both units was showed in Table 4.

Arduino IDE will be used as the software medium to reprogram, read and give instruction in IMU sensors. IMU will be program to give instruction for the microprocessor to send data collected into PC.

Table 4. Connection Pin Interfacing USB-UART and IMU

USB-UART Converter	ArduIMU+
Data Terminal Ready (DTR)	Auto-reset
Receiver (Rx)	Transmitter (Tx)
Transmitter (Tx)	Receiver (Rx)
Voltage (Vsel)	Input Voltage
Clear To Send (CTS)	Ground (GND)
Ground (GND)	Ground (GND) - BLK

### 3.4 Data Post Processing

Simulink MATLAB will be applied for data post processing to visualize results collected from IMU sensor in the form of graphs. The data will be read through MATLAB to come out with graph form. The dimension of the graph will be based on Acceleration / Gyro results over a distance (KM). Recorded data will be compared in order to get any differences in railway vibration results. Figure 7 shows the example of graphical output (Acceleration Z-axis vs Distance) that should be visualized after data post processing.

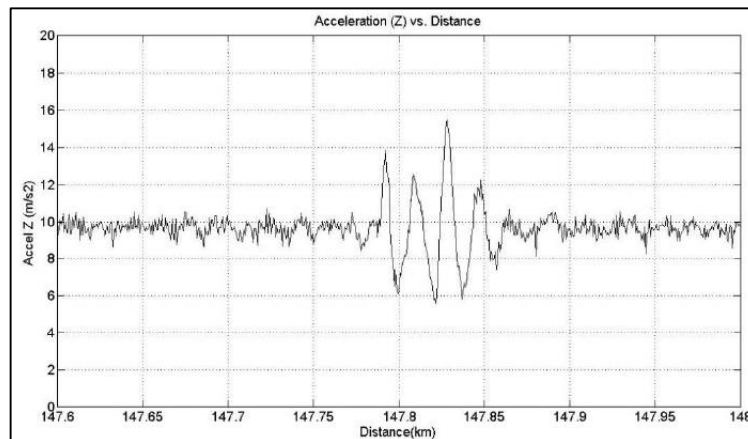


FIGURE 7. Example of Output (Graph)



### 3.5 Hardware-Software Interface

The driver for USB-UART converter need to be installed before it was successfully connected into a PC system by showing its connection on USB Serial Port. As the Arduino ATmega328 Microcontroller already built in in IMU sensor, thus the interfacing between IMU and PC could be programmed by using Arduino IDE. MPU-6000 library was also added into Arduino IDE, libraries and programmed to obtain raw data from IMU sensor.

The IMU sensor was put on a level surface and baud rate was set at 38400. The simple information from these sensors were sent at the clock rate of 1MHz and the example rate of around 50Hz by utilizing Serial Peripheral Interface (SPI). The program stream diagram was appeared as in Figure 8.

### 3.6 Direct Cosine Matrix (DCM) Algorithm

Execution of direct-cosine-framework (DCM) calculation in the framework keeping in mind the end goal to acquire the helpful orientation development from the raw data information. DCM works in three imperative ways; which is the gyroscope was utilized as the essential wellspring of introduction data. Perceiving the numerical blunders in the combination by utilizing reference vectors. A proportional plus integral (PI) feedback controller was implemented in order to gain the fed back and make necessary adjustment to the matrix system in DCM. Figure 8 underneath demonstrates the piece outline of DCM.

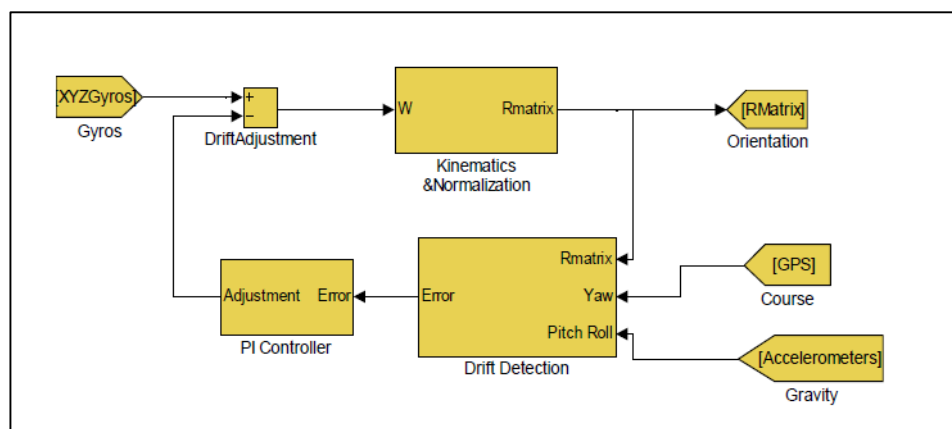


FIGURE 8. Direct Cosine Matrix (DCM) Algorithm Block Diagram

As it concerned with rotation, DCM algorithms can be used to represent the orientation of moving train with respect to the ground frame. Thus it applied 9

elements of rotation matrix which is used to describe the orientation of one coordinate with respect to another. As the properties of rotation matrix when the body and ground coordinates in perpendicular position, thus the row and column are supposed to be in perpendicular to each other and the output from the squares of these elements is equal to 1.

$$Rotation\ Matrix = \begin{bmatrix} r_{xx} & r_{xy}/G_{-z} & r_{xz}/G_y \\ r_{yx}/G_z & r_{yy} & r_{yz}/G_{-x} \\ r_{zx}/G_{-y} & r_{zy}/G_x & r_{zz} \end{bmatrix} \quad (1)$$

The acceleration motion on the train are represented as  $r_{xx}$ ,  $r_{yy}$ , and  $r_{zz}$  ( $m/s^2$ ) while the three-Euler angles are labeled as  $G_x$ ,  $G_y$ , and  $G_z$  (radians per second) as shown in rotation matrix above. Normalization process is required to keep the orthogonality conditions as formulate in Equation (1) by the dot product of the X and Y rows of the matrix, as described in Equation (2).

$$Error = X.Y = X^T Y = \begin{bmatrix} r_{xx} & r_{xy} & r_{xz} \end{bmatrix} \begin{bmatrix} r_{yx} \\ r_{yy} \\ r_{yz} \end{bmatrix} \quad (2)$$

Half of the error was allocate to each X and Y rows after defining the orthogonality error in Equation (2) by using the formula in Equation (3) and (4).

$$\begin{bmatrix} r_{xx} \\ r_{xy} \\ r_{xz} \end{bmatrix}_{orthogonal} = X_{orthogonal} = X - \frac{error}{2} Y \quad (3)$$

$$\begin{bmatrix} r_{yx} \\ r_{yy} \\ r_{yz} \end{bmatrix}_{orthogonal} = Y_{orthogonal} = Y - \frac{error}{2} X \quad (4)$$

While Z row will be adjusted to be orthogonal by using cross product of the X and Y as formulate in Equation (5) below.

$$\begin{bmatrix} r_{zx} \\ r_{zy} \\ r_{zz} \end{bmatrix}_{orthogonal} = Z_{orthogonal} = Y_{orthogonal} * X_{orthogonal} \quad (5)$$

And the last step of the normalization of the rotation matrix is to adjust the magnitude of each row vector to one. Thus, the formula in Equation (6) was used for scaling X row and the same applied to Y and Z rows.

$$X_{normalized} = \frac{1}{2}(3 - X_{orthogonal} \cdot X_{orthogonal})X_{orthogonal} \quad (6)$$

To recognize gyro drift adjustment, in this way the usage of reference vectors from accelerometers were utilized to distinguish and to give a negative feedback loop back to the gyros. As appeared in Equation (7), the orientation error was planned by utilizing cross result of the deliberate vector with the vector evaluated by DCM. The Euler edges can be computed in view of the recipe appeared in Equation (8), (9), and (10).

$$Error_{roll,pitch} = Acceleration_x r_{zx} \quad (7)$$

$$Pitch = -\sin^{-1}r_{zx} \quad (8)$$

$$Roll = atan2(r_{zy}, r_{zz}) \quad (9)$$

$$Yaw = atan2(r_{yx}, r_{xx}) \quad (10)$$

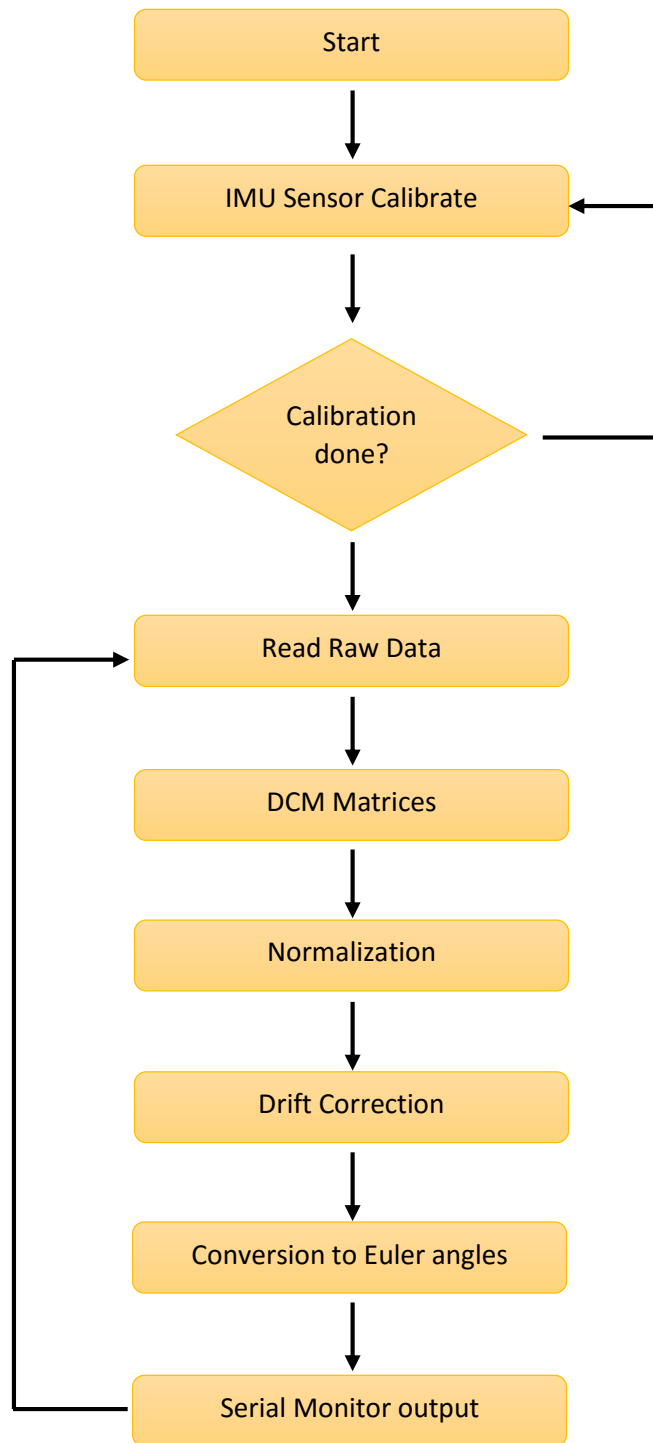


FIGURE 9. Program flowchart representing the workflow of interfacing between PC and IMU

## CHAPTER 4

### RESULT AND DISCUSSION

#### 4.0 Output Data

Few test has been done a few times to see the interface between IMU and USB-UART converter successfully connected. By using Arduino IDE, the data can be displayed on Serial Monitor as shown in Figure 9. By setting up into 38400 baud, the data will be displayed in six readings which is tri-axis acceleration and tri-axis gyros. The collected data will be captured and saved into a text file (.txt) and later being extracted into Excel file (.csv or .xls).

MATLAB will be used for post-processing and analysis. Figure 10 and Figure 11 shows the sample data being collected and stored in .txt and .xls format. By saving all these data into a PC, the user can review and post-process the data. The travel distance for each data was estimated with the assumption of constant velocity.

Data	Roll	Pitch	Yaw	Acceleration(x)	Acceleration(y)	Acceleration(z)
1	-0.01	0.01	0.00	0.00	-0.17	9.91
2	-0.07	0.02	-0.04	0.01	0.04	9.88
3	-0.11	0.02	-0.10	0.00	0.23	9.94
4	-0.08	-0.01	-0.11	-0.00	0.23	9.82
5	0.01	-0.05	-0.08	0.01	0.01	9.62
6	0.05	0.01	-0.07	-0.02	-0.33	9.78
7	-0.05	0.05	-0.12	0.01	-0.15	9.94
8	-0.15	0.07	-0.21	0.05	0.15	9.98
9	-0.14	0.07	-0.27	0.06	0.23	9.89
10	-0.03	0.07	-0.26	0.00	-0.07	9.71
11	0.01	0.08	-0.25	0.03	-0.20	9.67
12	-0.02	0.11	-0.29	0.01	-0.17	9.76
13	-0.09	0.14	-0.36	0.05	0.02	9.90
14	-0.08	0.17	-0.41	0.06	0.17	9.80
15	0.02	0.21	-0.41	0.05	0.01	9.79
16	0.08	0.26	-0.41	0.06	-0.10	9.80
17	0.05	0.30	-0.47	0.09	0.03	9.95
18	0.02	0.32	-0.54	0.10	0.17	9.97
19	0.03	0.31	-0.59	0.09	0.25	9.89
20	0.09	0.30	-0.60	0.09	0.20	9.84
21	0.17	0.29	-0.58	0.06	-0.12	9.80
22	0.14	0.27	-0.58	0.08	-0.11	9.76
23	0.08	0.27	-0.62	0.07	0.04	9.81
24	0.06	0.28	-0.66	0.07	0.15	9.85
25	0.11	0.30	-0.66	0.09	0.03	9.76
26	0.12	0.33	-0.66	0.10	0.03	9.92
27	0.14	0.36	-0.67	0.09	-0.02	9.97
28	0.14	0.35	-0.68	0.09	-0.01	9.96
29	0.09	0.31	-0.72	0.10	0.20	9.77
30	0.09	0.28	-0.73	0.10	0.27	9.78

FIGURE 10. Output Data on Serial Monitor

Data	Roll	Pitch	Yaw	Acceleration(x)	Acceleration(y)	Acceleration(z)
1	0.02	-0.05	-0.17	-0.18	0.59	9.92
2	0.19	-0.12	-0.22	-0.18	0.51	9.80
3	0.35	-0.11	-0.27	-0.19	-0.03	9.49
4	0.19	-0.04	-0.40	-0.20	0.23	9.63
5	-0.06	0.07	-0.55	-0.16	0.62	9.84
6	0.01	0.13	-0.58	-0.33	0.10	10.25
7	0.07	0.10	-0.62	-0.34	-0.14	10.13
8	-0.06	0.01	-0.74	-0.21	0.31	9.86
9	-0.02	-0.06	-0.87	-0.31	0.48	9.47
10	-0.08	0.10	-0.90	-0.27	0.88	9.40
11	-0.07	0.40	-0.83	-0.38	0.47	10.34
12	0.06	0.57	-0.75	-0.29	0.01	10.59
13	0.08	0.50	-0.77	-0.36	0.53	9.52
14	0.11	0.46	-0.77	-0.25	0.68	9.23
15	0.15	0.59	-0.72	-0.35	0.34	9.63
16	0.06	0.74	-0.65	-0.38	0.18	10.28
17	-0.07	0.70	-0.72	-0.28	0.51	9.66
18	-0.12	0.71	-0.78	-0.35	0.84	9.55
19	-0.04	0.78	-0.77	-0.38	0.81	9.74
20	0.05	0.82	-0.69	-0.43	-0.28	10.02
21	-0.20	0.81	-0.78	-0.30	0.27	9.79
22	-0.44	0.83	-0.93	-0.28	0.96	9.59
23	-0.45	0.91	-0.97	-0.36	1.02	9.68
24	-0.28	1.00	-0.91	-0.38	-0.07	10.22
25	-0.43	1.00	-0.95	-0.38	0.05	9.81
26	-0.64	0.99	-1.08	-0.30	0.66	9.58
27	-0.71	1.16	-1.05	-0.33	0.67	10.06

FIGURE 11. Output Data in Text File (.txt)

Data	Roll	Pitch	Yaw	Acceleration(x)	Acceleration(y)	Acceleration(z)
1	0.02	-0.05	-0.17	-0.18	0.59	9.92
2	0.19	-0.12	-0.22	-0.18	0.51	9.8
3	0.35	-0.11	-0.27	-0.19	-0.03	9.49
4	0.19	-0.04	-0.40	-0.20	0.23	9.63
5	-0.06	0.07	-0.55	-0.16	0.62	9.84
6	0.01	0.13	-0.58	-0.33	0.1	10.25
7	0.07	0.10	-0.62	-0.34	-0.14	10.13
8	-0.06	0.01	-0.74	-0.21	0.31	9.86
9	-0.02	-0.06	-0.87	-0.31	0.48	9.47
10	-0.08	0.1	-0.9	-0.27	0.88	9.4
11	-0.07	0.4	-0.83	-0.38	0.47	10.34
12	0.06	0.57	-0.75	-0.29	0.01	10.59
13	0.08	0.5	-0.77	-0.36	0.53	9.52
14	0.11	0.46	-0.77	-0.25	0.68	9.23
15	0.15	0.59	-0.72	-0.35	0.34	9.63
16	0.06	0.74	-0.65	-0.38	0.18	10.28
17	-0.07	0.7	-0.72	-0.28	0.51	9.66
18	-0.12	0.71	-0.78	-0.35	0.84	9.55
19	-0.04	0.78	-0.77	-0.38	0.81	9.74
20	0.05	0.82	-0.69	-0.43	-0.28	10.02
21	-0.2	0.81	-0.78	-0.3	0.27	9.79

FIGURE 12. Output Data in Excel File (.xls)

## 4.1 Lab Testing

Lab testing has been done in the process to validate the sensor into its optimum validation, and to seek its percentage error compare to other sensors for differentiating its accuracy and reliability. Figure 12 is the Vibration Shaker that is used in the process to give certain vibrations in some set up frequency (Hz) and acceleration ( $m/s^2$ ). Few test has been done in some different ways to study the differences between each output for further analysis and study. The vibration shaker was set up in two ways which is Sweep Process and Spot Process. Sweep Process is a process when the frequency was set up for low to high value (Hz) in constant gravitational acceleration ( $9.81 m/s^2$ ) while Spot Process is another process to capture the data in constant frequency versus constant gravitational acceleration ( $m/s^2$ ).



FIGURE 13. Vibration Shaker

### 4.1.1 Equipment Setup

Prototype platform was designed in order to obtain the data in 3-axis surfaces. As the vibration shaker can give output in vertical vibration, thus the experiment need to be set up in 3-axis interfaces. Figure 13 below is the platform to hold the sensor during the testing.

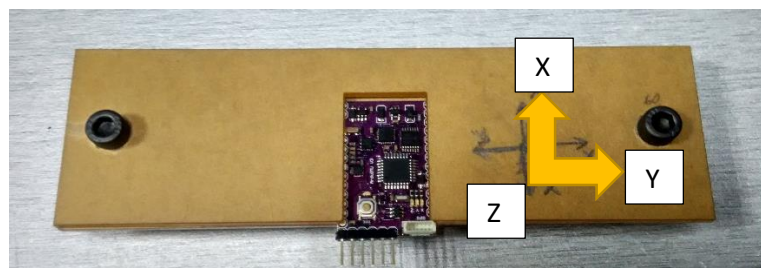


FIGURE 14. Prototype Platform

The sensor will be placed in 3 different ways in order to get each axis acceleration during the testing. As for z axis, the sensor will be placed shows in Figure 14 below. While Figure 15 and Figure 16 shows the interface for x axis and y axis. Once the sensor was set up as the figures below, thus the equipment need to run few configurations in order to set the value of frequency (Hz), acceleration ( $m/s^2$ ) and time (minutes).

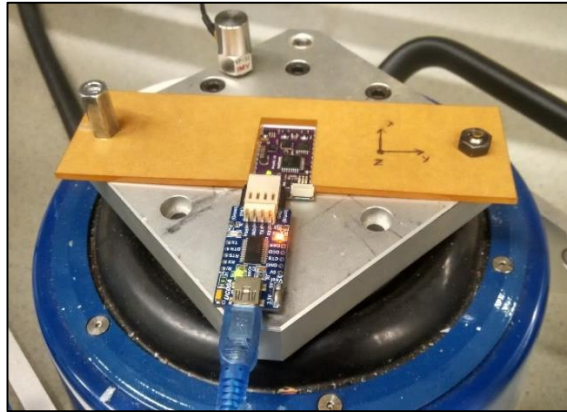


FIGURE 15. Z Axis Interface

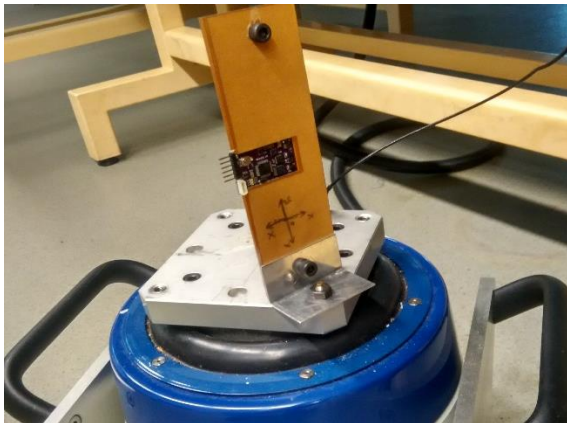


FIGURE 16. Y Axis Interface

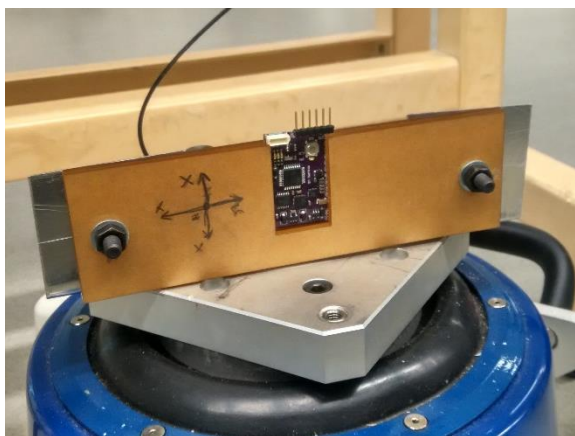


FIGURE 17 X Axis Interface



Thus, the equipment will start to operate as it configured for the data collection. As from the Figure 17 below shows the example of interface for testing frequency 20 Hz with constant acceleration, 9.81 m/s<sup>2</sup>. Once the full cycles done, the shaker will be automatically stop.

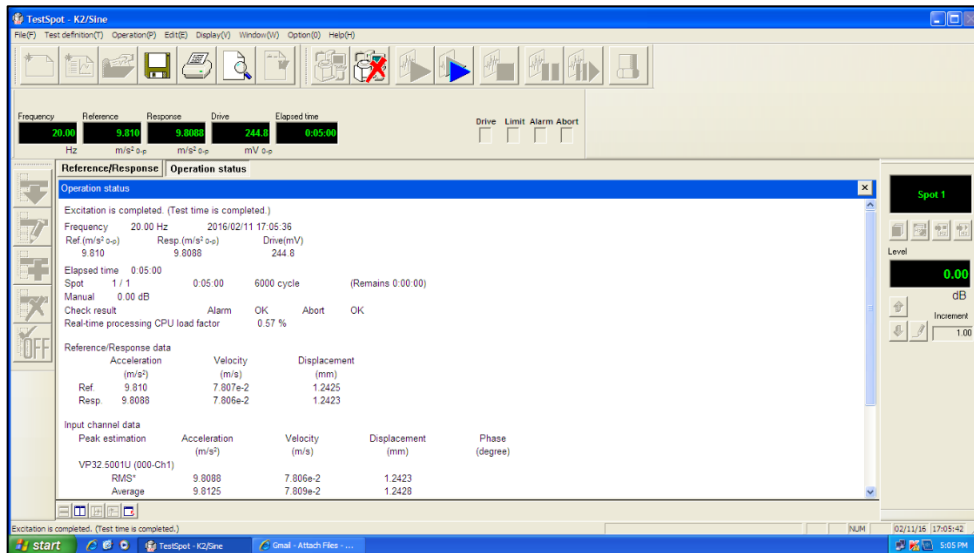


FIGURE 18. Software Interface 20 Hz

#### 4.1.2 Data Collection/ Result Discussion

Data collection was collected in three (4) different ways in order to see any changes of the vibration data patterns. Different frequency with different magnitude has been collected which is high frequency with constant magnitude (1 G), low frequency with constant magnitude, and low frequency with different magnitude; low and high. This lab testing was made in order to see either different magnitude could affect the reading of the sensor itself, so that analysis can be made. Together with the different values of frequency because somehow the train itself could create low frequency every time there is some misalignment or low quality of the track itself. Last but not least, the system will be placed in z axis with 0 Hz was applied to see the raw data with no vibration applied on it. Thus it can help in validate this application before the real testing on train.

## High Frequency Vibration (100Hz-180Hz)

Here are the lab testing from 100Hz – 180 Hz with a constant value of acceleration (9.81 m/s<sup>2</sup>). From the graph itself, it shows that each axis in sine wave formation. As in Figure 18, the sensor was placed in z axis orientation, which creates more constant form in z axis compare to both y axis and z axis. Same goes to y axis graph in y axis orientation (Figure 19) as the graph shows more constant form compare to z axis and x axis.

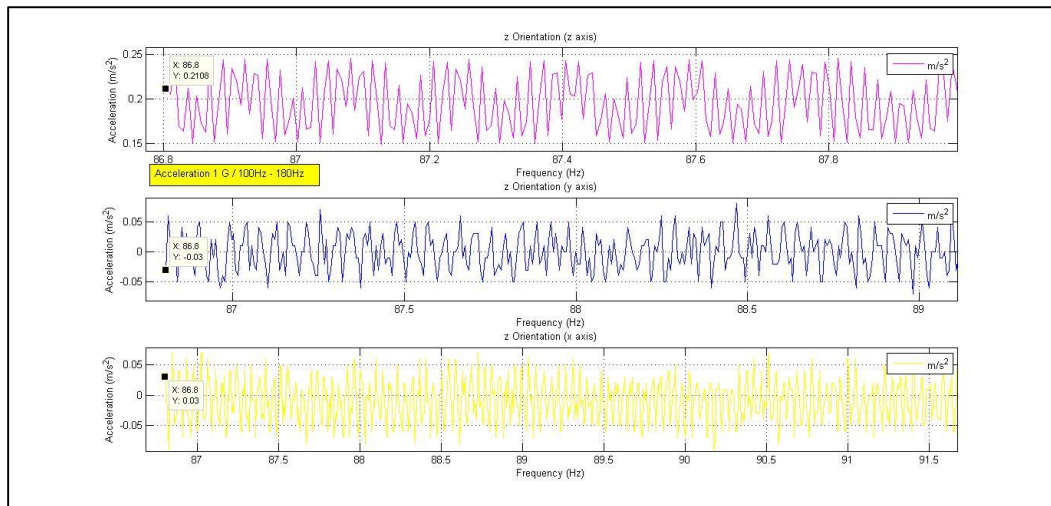


FIGURE 19. z Orientation ( 1G )

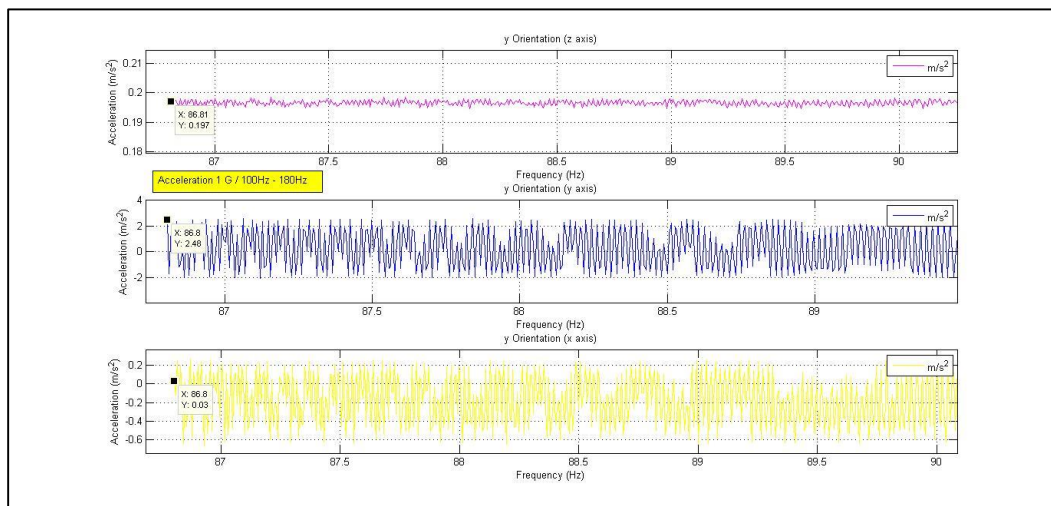


FIGURE 20. y Orientation ( 1G )

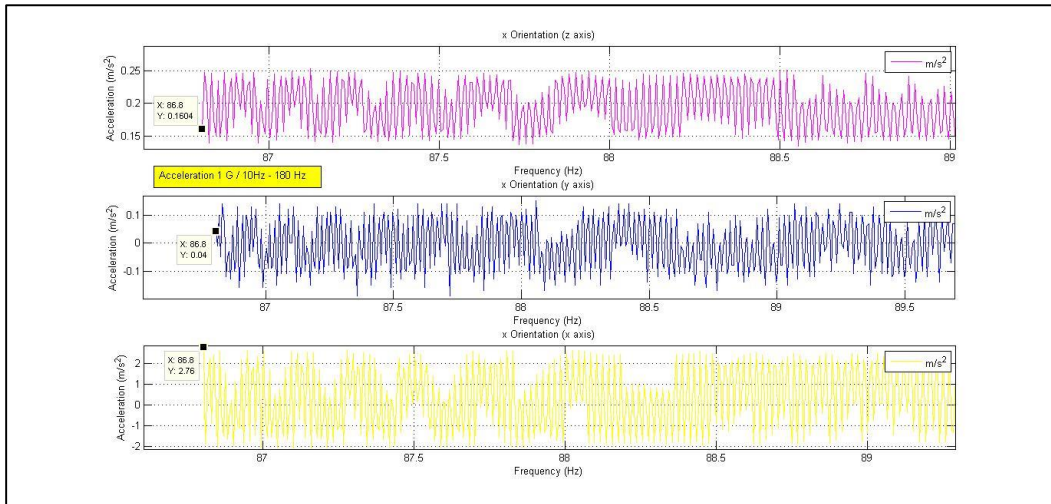


FIGURE 21. x Orientation ( 1G )

### Low Frequency Vibration (5Hz-20Hz)

While in this part will be elaborated in constant acceleration ( $9.81 \text{ m/s}^2$ ) but now in low value of frequency starting 5Hz – 80Hz. As low frequency could create high movement in certain displacement, thus each output from each axis shows the higher starting value in the range of  $9.00 \text{ m/s}^2$  -  $10.00 \text{ m/s}^2$ . As for the each axis from each orientation will give same output and the same form of vibration.

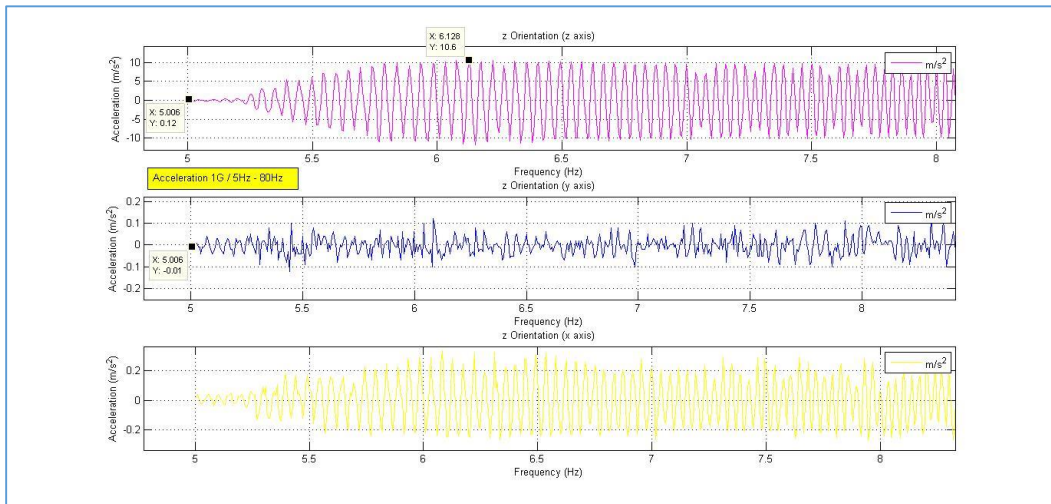


FIGURE 22. z Orientation ( 1G )

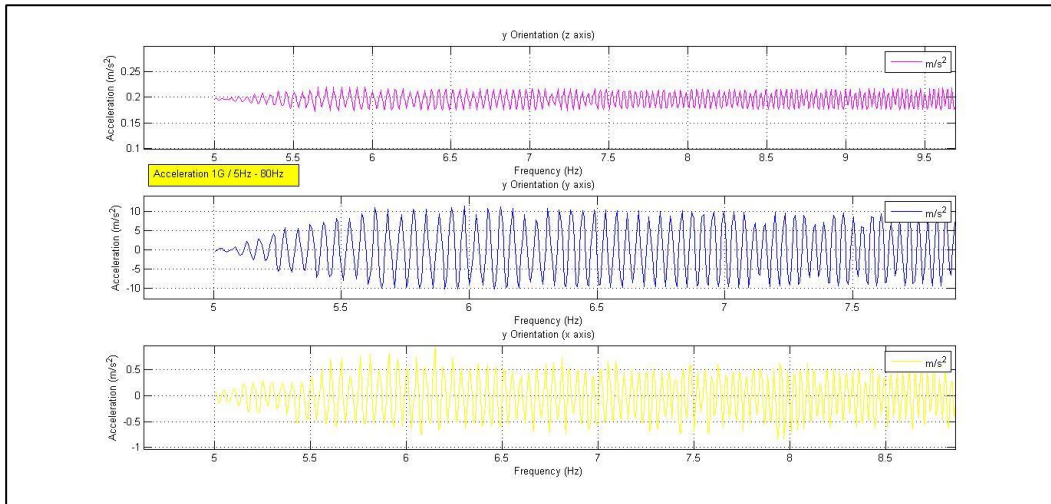


FIGURE 23. y Orientation ( 1G )

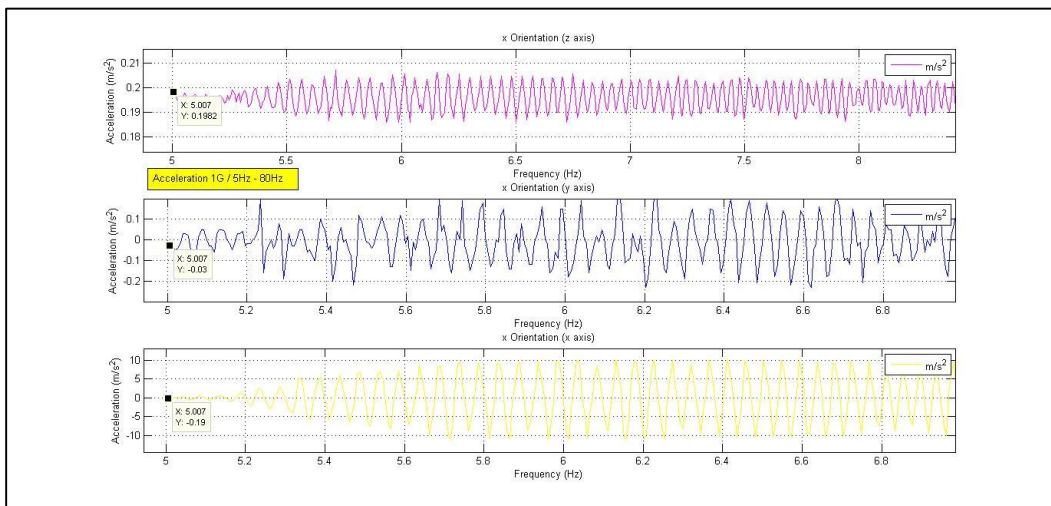


FIGURE 24. x Orientation ( 1G )

### Low Frequency versus High Magnitude (5Hz-20Hz)

Another testing was made in low frequency, but with different set of magnitude, which will be discussed on lowest and highest magnitude only. As the shaker could set up a minimum of 0.1 G until 1.5 G, so the limitation of testing the sensor in higher values of magnitude might affect the shaker itself. So in this part, 1.5 G magnitude ( $15.00 \text{ m/s}^2$ ) was tested on the sensor to see any changes on the vibration. As what the output shows in Figure 24, Figure 25 and Figure 26, the formation of the graph almost looks alike as compared with previous data.

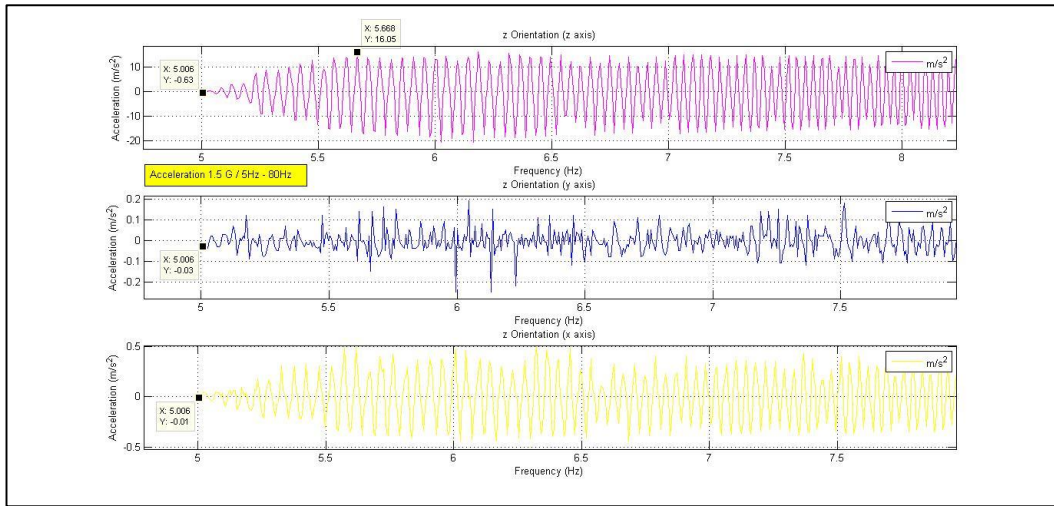


FIGURE 25. z Orientation ( 1.5G )

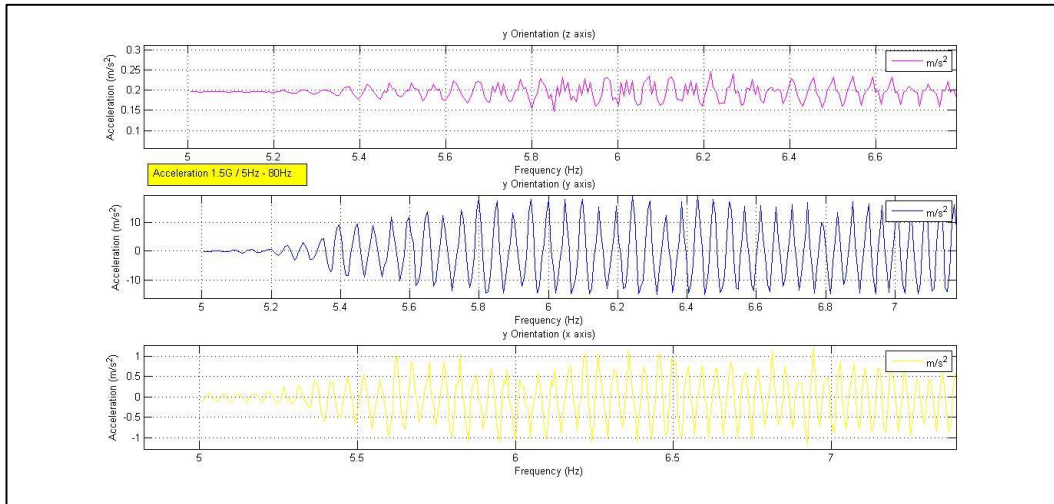


FIGURE 26. y Orientation ( 1.5G )

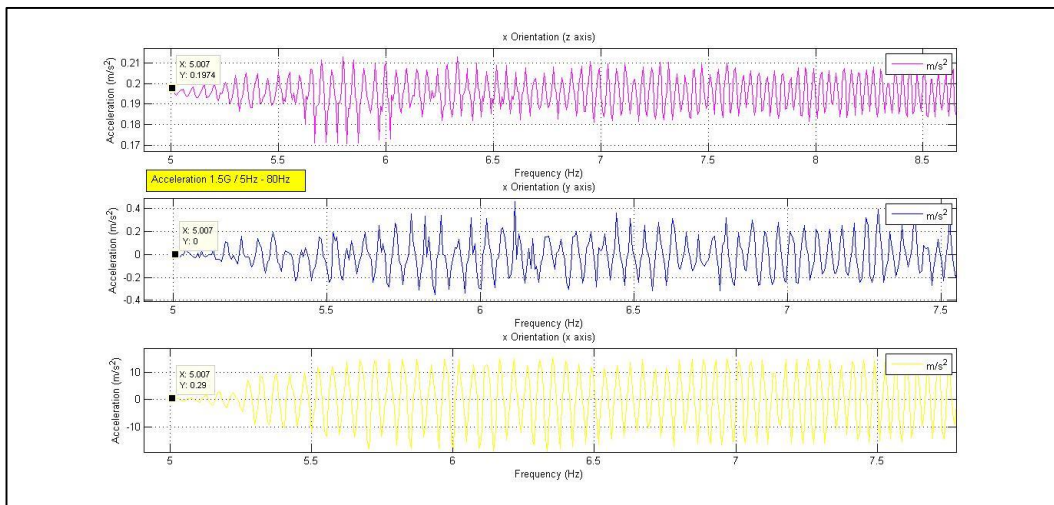


FIGURE 27. x Orientation ( 1.5G )

## Low Frequency versus Low Magnitude (5Hz-20Hz)

In this testing, the magnitude was set in minimum acceleration, which is 0.1G (0.981 m/s<sup>2</sup>). It can conclude that minimum acceleration could affect the readings which is much lower output compare to higher acceleration. As compared with graph patterns the highest magnitude is almost 0.3 m/s<sup>2</sup> compared to higher acceleration which is almost same as 9.81 m/s<sup>2</sup>.

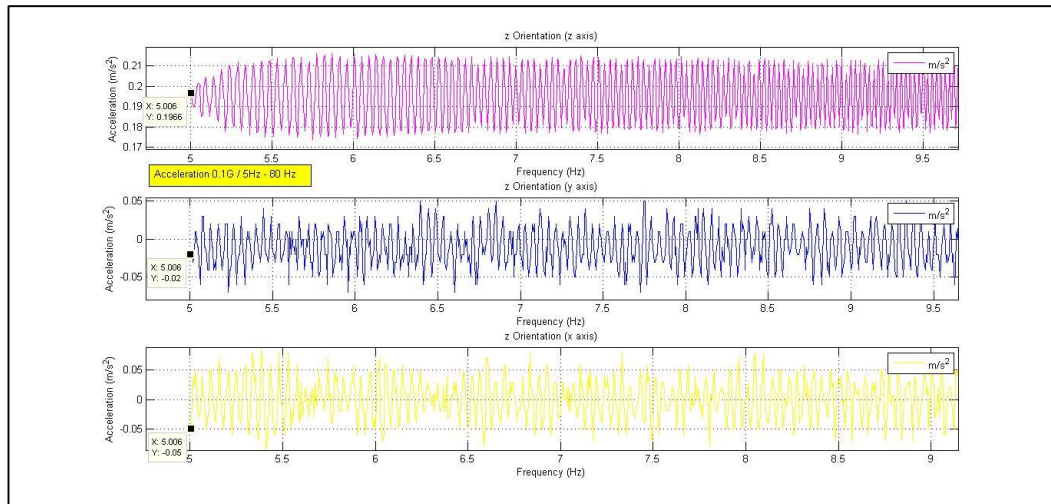


FIGURE 28. z Orientation ( 0.1G )

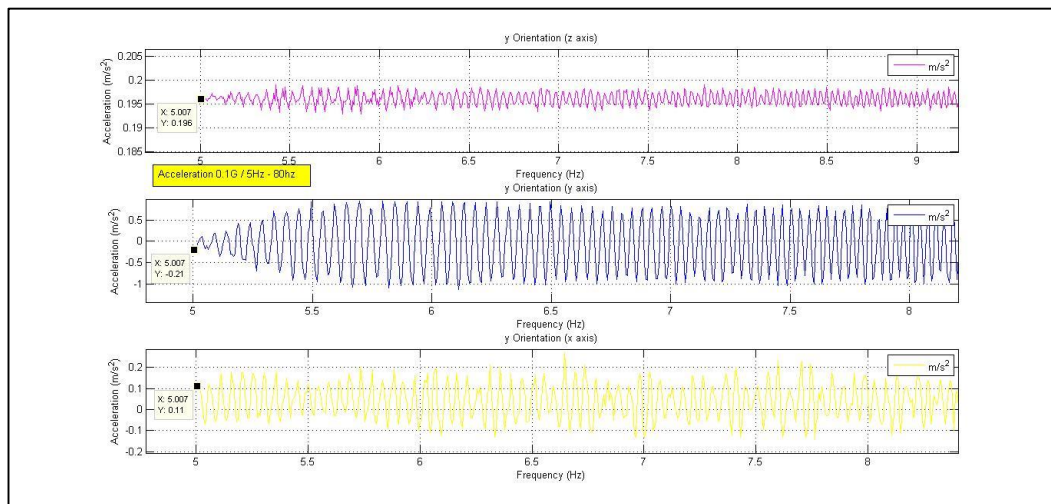


FIGURE 29. y Orientation ( 0.1G )

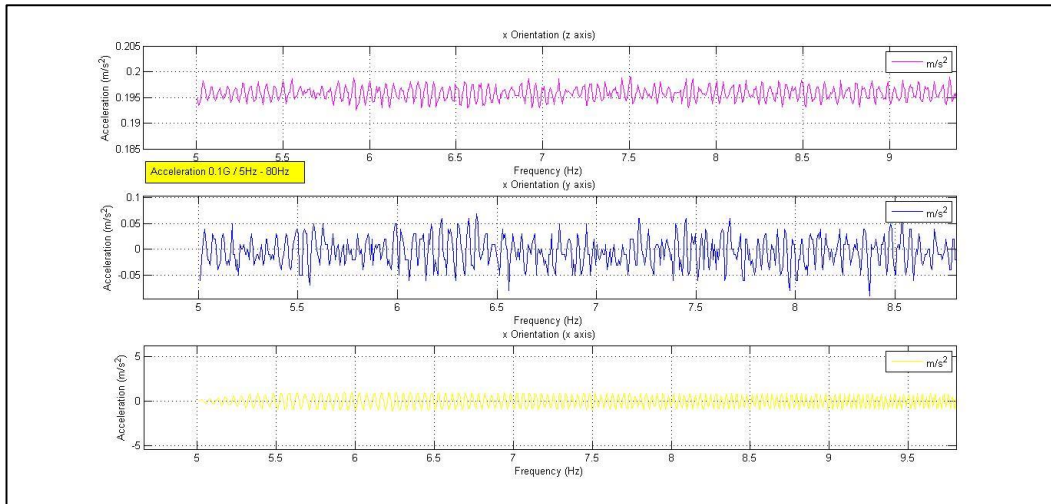


FIGURE 30. x Orientation ( 0.1G )

No Frequency (0 Hz) with Normal Magnitude

In this testing, the IMU sensor will be placed in z axis orientation when no frequency was applied to it. This testing's purpose is to see the raw pattern of the vibration in constant 0 Hz. As in Figure 31 below, all the axis were in constant form compared to previous data were all the graph shows any changes in the other axis while the exact orientation will show some constant form of vibration. Thus, it can conclude that the other axis which is not in their orientation will shows some differences in their vibration.

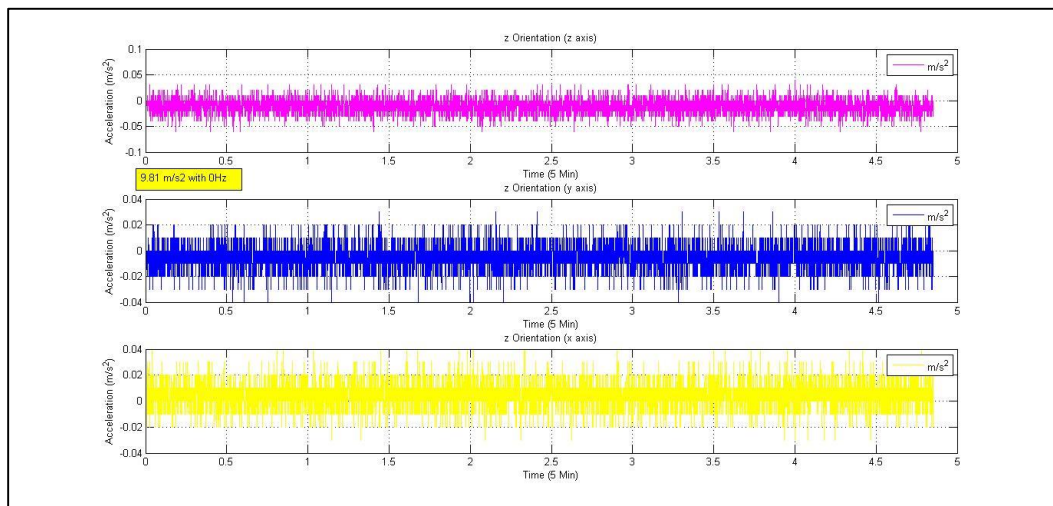


FIGURE 31. 0Hz Frequency

## 4.2 Car-mounted Field Testing

The prototype was placed at the top of the dashboard of a car and has been collecting data along the road in front of Chancellor Hall, UTP, as shown in Figure 32 below. The reason of having this testing to evaluate the capability of the prototype for detecting bumps on the road. The car type used is Myvi, at the distance approximately  $0.4\text{ km}$  at the range of average velocity around  $15\text{ km/h}$  to  $20\text{ km/h}$  within a duration of 1.04 minutes.

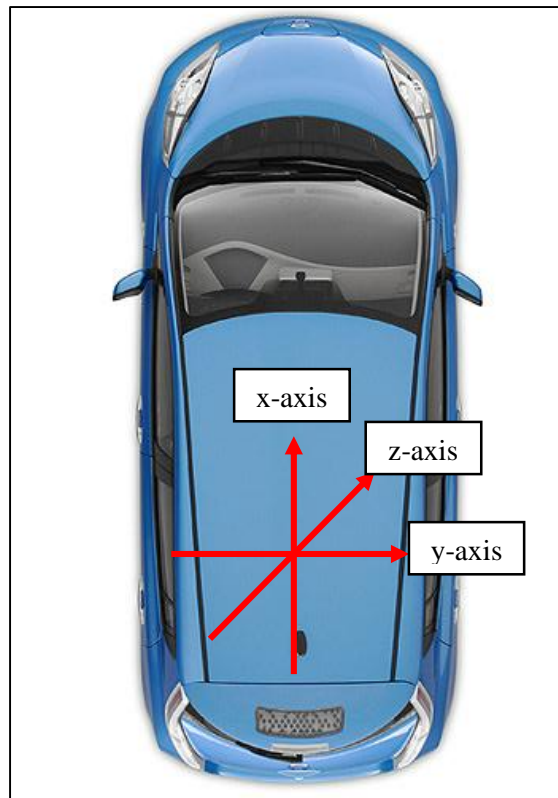


FIGURE 32. Axis Position

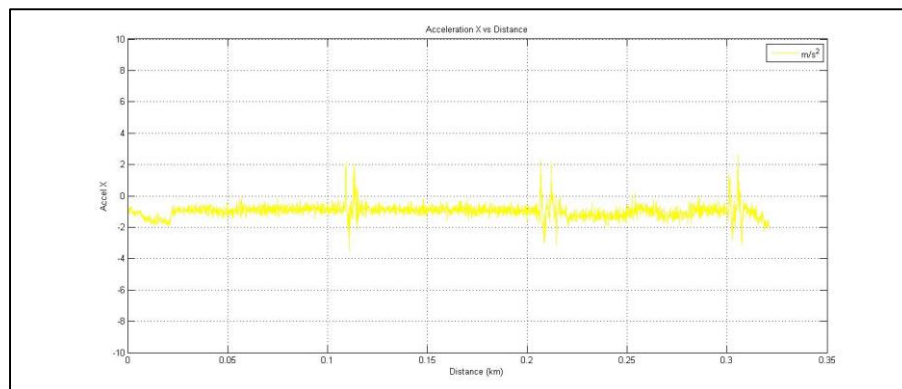


FIGURE 33. Car-Mounted Field testing (Bump)



From the data collected from the testing, approximately 2700 set of samples were collected and around 150 Kilobyte (KB) of data were saved onto PC system. 30 sets of samples were collected roughly per second and sampling distance of between 100 mm – 120 mm. Figure 33 below shows the overall collected data from the car testing which contains of three separated humps in average of 0.4 km distance. The location of the humps can be observe through the four graphs which is x-axis acceleration, y- axis acceleration, z-axis acceleration, and pitch angle where the differences of magnitude and vibration changes could be identified. But in this figure, it's clearly shows certain degree of vibration noise, which most probably due to the irregular running surfaces of vehicles, suspension system of the car, and could be noise created from the sensor itself. While the roll angles couldn't shows any significant views of changes in vibration itself, due to noise present on the signal.

As x-axis acceleration shows the motion of backward and forward direction, while y-axis acceleration for horizontal motion which is right and left direction, and z-axis direction for upward and downward direction. A low-pass filter will be applied to improve the signal to noise ratio (SNR). Then, to differentiate and eliminate the high-frequency noise as the low motion of the vibration created by the car when it passes through an obstacle or hump.



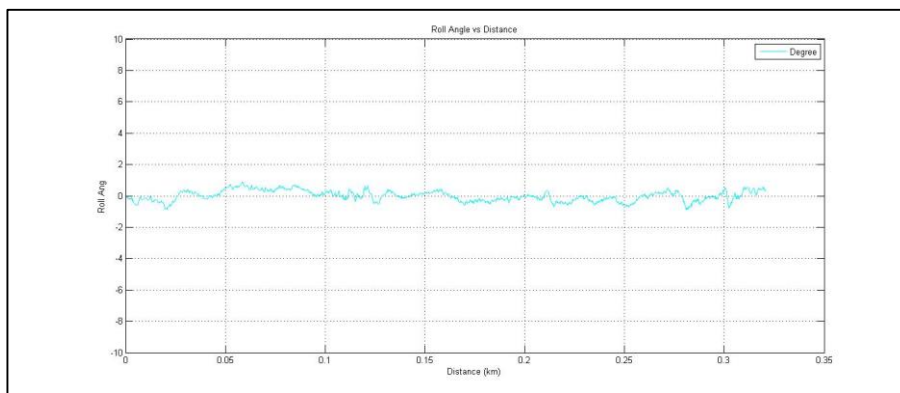
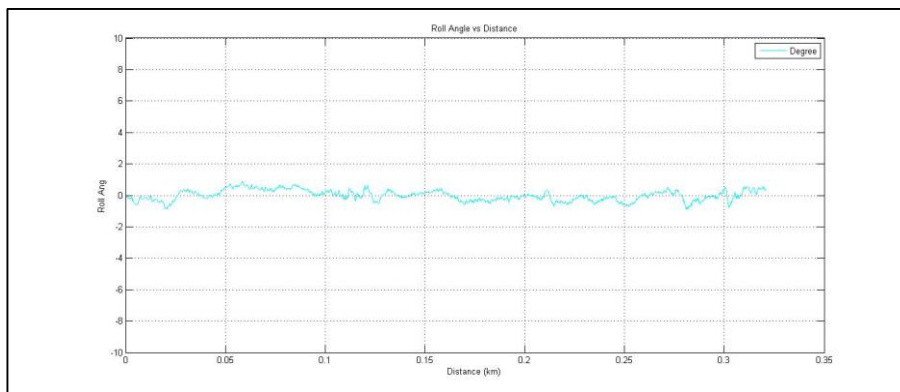
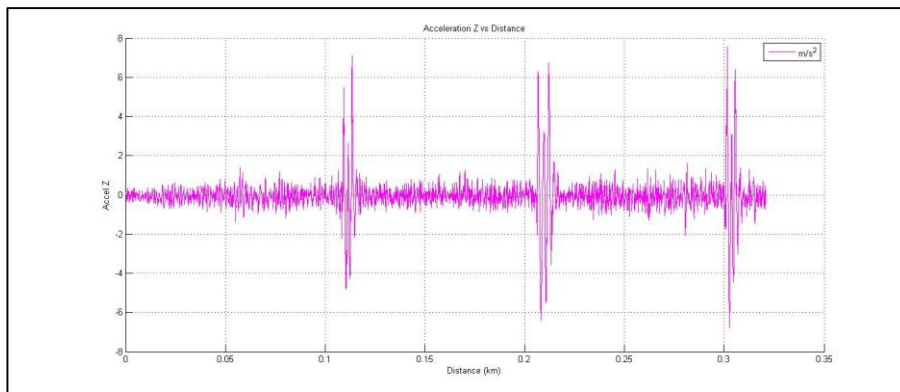
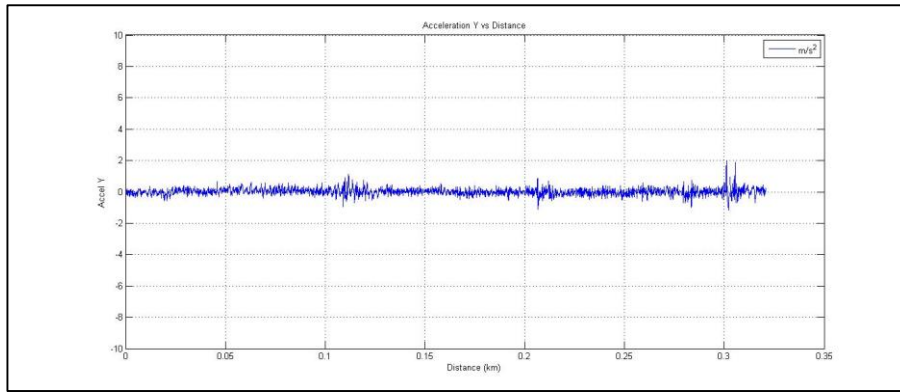


FIGURE 34. Collected IMU data for car-mounted field testing over distance

As what has been shown in Figure 34 above, where the observation can be made as there is a significant views in the z-axis acceleration and x-axis acceleration as it shows higher sensitivity compared to y-axis acceleration when it lift up through the hump. This due to the y-axis motion is for left and right, the spikes from this axis probably due to the low frequency of the sensor when it comes into bump. Maximum acceleration that can occurred upon reaching the hump will be around  $7.1 \text{ m/s}^2$  while the maximum pitch angle is approximately around  $2^\circ$ , when the car is going to lift up through the hump. Multiple spikes could be identified in x-axis acceleration as shown in Figure 34, due to noise created due to motion distortion. As it may happens due to orientation overflow and displace from its ground platform when it pass through the hump, it may create some spikes as it record predisposed value of acceleration.

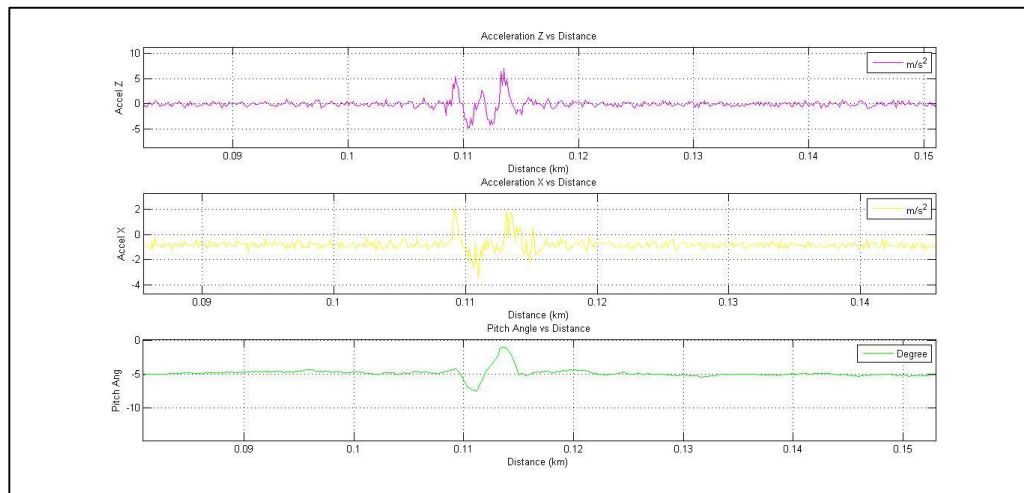


FIGURE 35. Close-up on pitch angle, x-axis acceleration and z-axis acceleration as car passes through second bump.

Low-pass filter is used in order to improve the signal to noise ratio as the measurements recorded contain different sources of vibration due to several factors. Finite Impulse Response (FIR) filter with stopband frequency of 1 Hz is used for this improvement. As shown in Figure 35, the car movement could be identified clearly after the filtering has been applied in the system.

Figure 35 shows that the car-mounted testing with filter was applied into it, and proved that the filtering technique could help in eliminating the noises, thus improve the signification of the car motion. While passing through the humps, it was believed that there will be small shaking created in terms of swinging motion of the car, however, due to its suspension system as shown in Figure 34, the motion probably affected by the variance of noises.

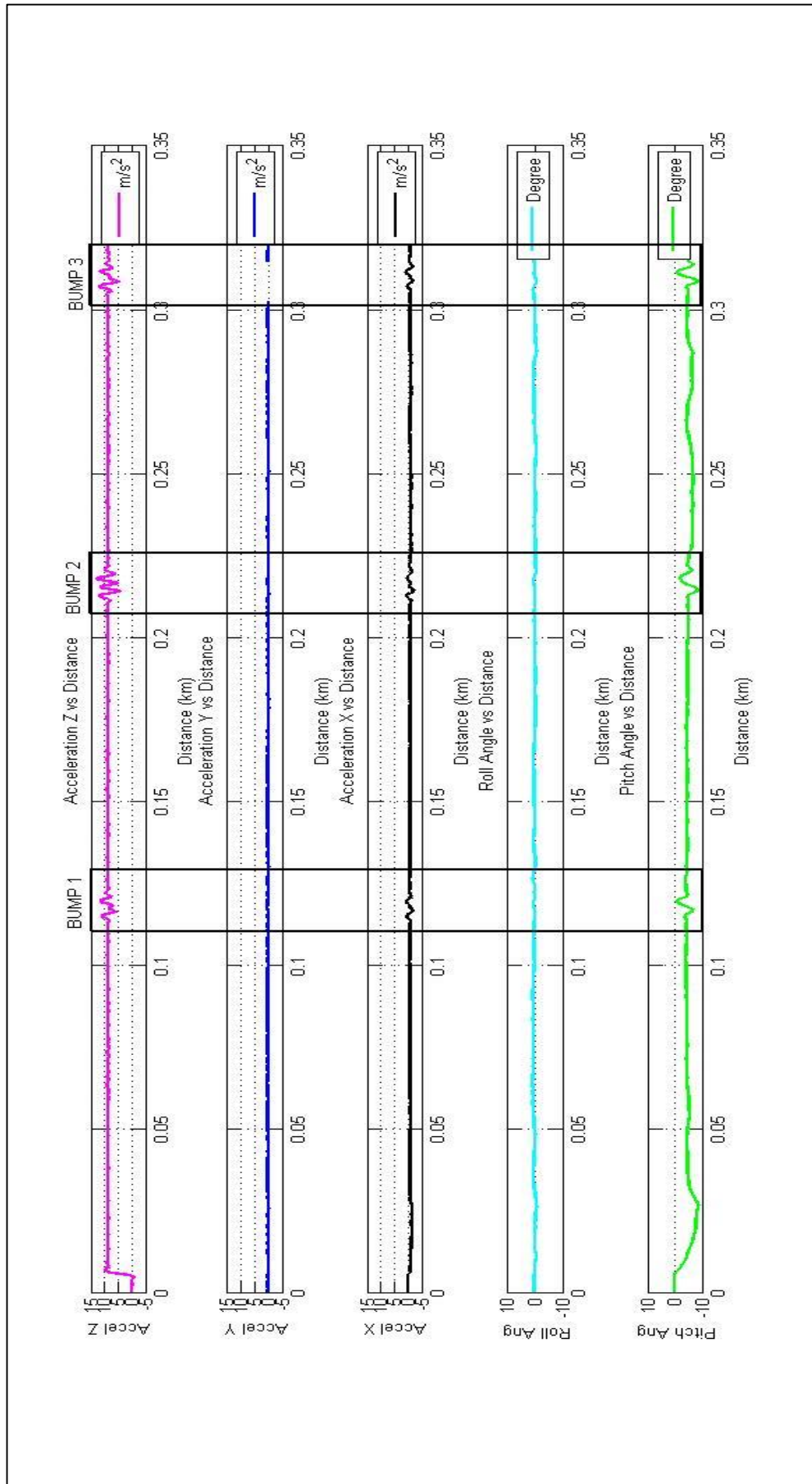


FIGURE 36. Collected IMU data for car-mounted field testing over distance (FIR)

By implementing this filter, both roll angle and y-axis acceleration can be improved by eliminating the high dynamic noise and vibration. As in Figure 33, both roll angle and y-axis acceleration shows the most high frequency noises, probably due to the low motion created. Thus it helps in detecting the low dynamics of car motion due to bumping surface. As what can be conclude, low-pass filter can be implement in way of better visualization and identification of rough road surfaces. Few improvement can be made, by using different types of filter, and different kind of road surfaces to see difference types of visualization created.

### 4.3 Train-mounted Field Testing

The testing has been made on a two direction inter-city train track of Electric Train Services (ETS) by Keretapi Tanah Melayu Berhad (KTMB). The system was set up in Batu Gajah station and need to initialize and few testing need to be conducted in order to make sure the sensor is working. The testing was covered from Kampar Station to Kuala Lumpur Station., which has a distance approximately around 220 km. Along this road, it combined of several type of railway environments, such as rural area, tunnel, city station and fast track section.



FIGURE 37. KTM Stations from Batu Gajah to Kuala Lumpur

As in Figure 37 shows the eight stations starting from Kampar Station to Kuala Lumpur Station. The system was taped on the floor of the passenger cabin, which at the first coach train (A). The data collected represents both conditions of passenger-loaded train and normal operating.

Around 15 MB were saved onto PC system and 300,000 of samples were collected via serial terminal. Figure 37 represents the collected data from Kampar Station to Kuala Lumpur Station. The distances pointed were estimated by assumptions as the train was travelled in constant speed of 105 km/h. Future implementation for the next improvement could be GPS module for the actual distance and location.

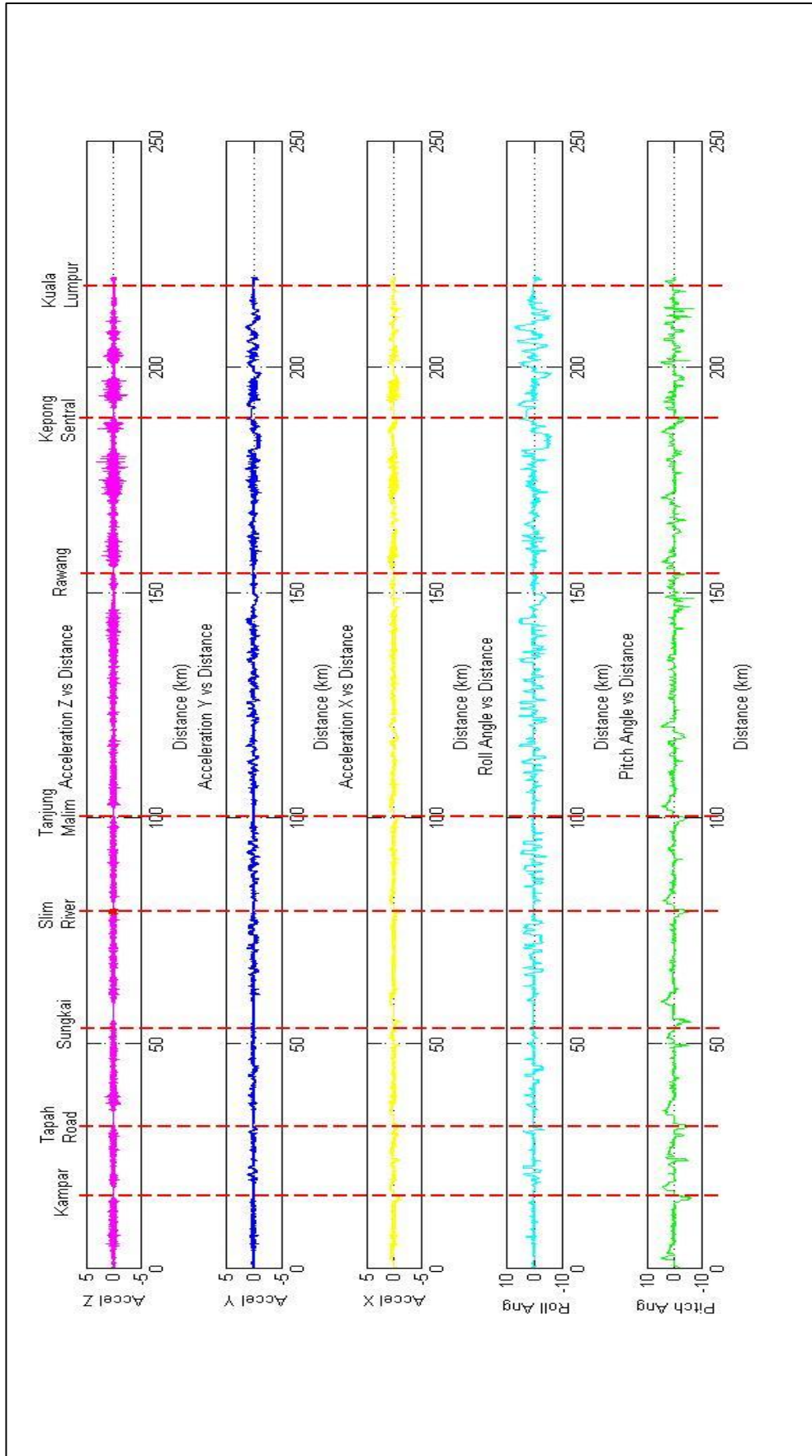


FIGURE 38. Collected IMU data for train-mounted field testing, covering from Kampar Station to KL Sentral Station

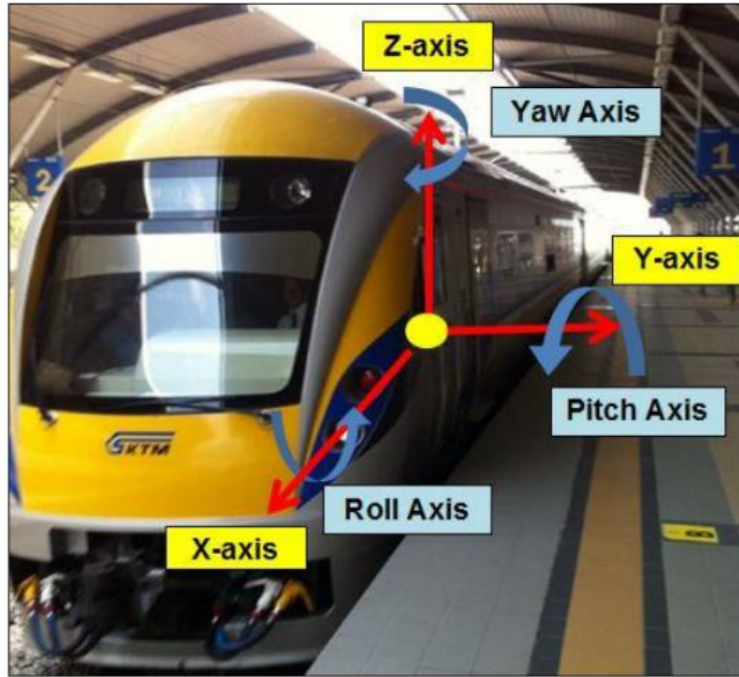


FIGURE 39. Axis Position

The location of each stations were collected approximately by following the constant velocity, 105 km/h.

Table 5. Approximately distance for each station

Station	Approximately Distance
Kampar	16.27 km
Tapah Road	31.69 km
Sungkai	53.34 km
Slim River	75.81 km
Tanjung Malim	96.53 km
Rawang	152.57 km
Kepong Sentral	188.09 km
Kuala Lumpur	210 km

#### 4.3.1 Overall Measurement System

Calibration of the IMU sensor were done during initialization, as it was mounted on track starting at Kampar Station. Overall observation were collected in Figure 38, as the z-axis acceleration (vertical movement) of the train were visualized and shows some changes on the vibration movement at from Rawang station to Kuala Lumpur

Station (  $153 \text{ km/h} - 210 \text{ km/h}$ ). Average acceleration that the train could obtain in steady motion and smooth is around  $0.91 \text{ m/s}^2$  to  $1.15 \text{ m/s}^2$ . But it starts to show some changes on the vibration movement at the distance of Rawang Station to Kuala Lumpur Station when the minimum acceleration was ( $-0.31 \text{ m/s}^2$ ) up to  $3.18 \text{ m/s}^2$  in maximum reading. From this observation, it actually shows some agreements as few people has been asks regarding the vibration created on this area, and it may affects the people as these places were actually hotspot for urbanization. It may affects the track from any misalignment due to the heavy and full-time usage of passengers.

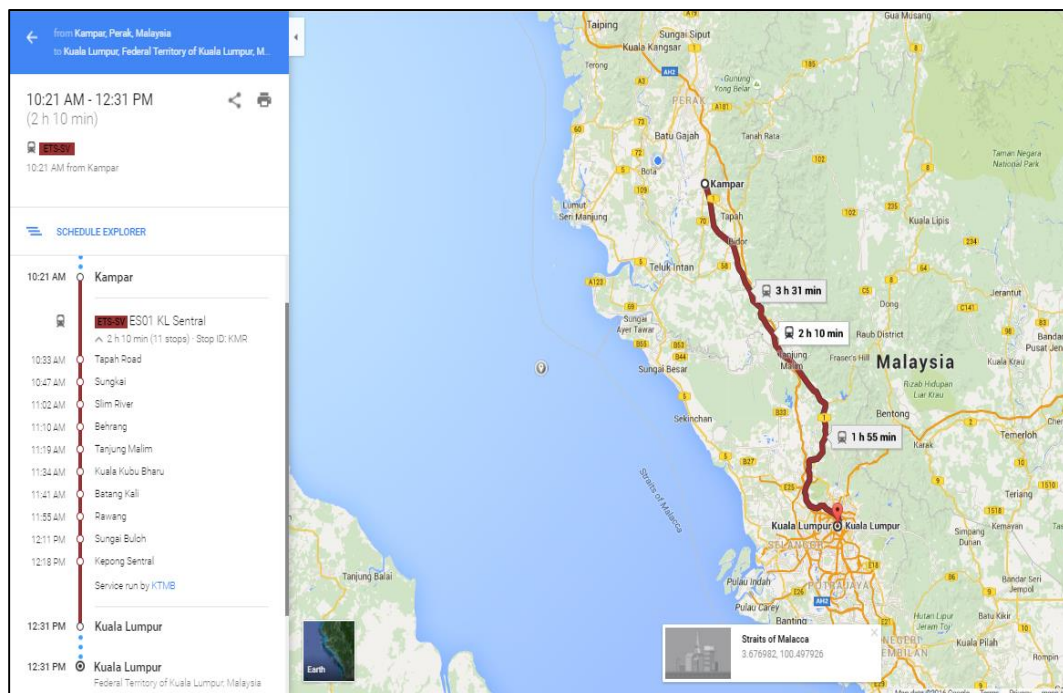


FIGURE 40. Distance coverage for train-mounted field testing

The left and right motion of the train could be observed through y-axis acceleration. As every movement of the train probably could create some left and right motions while slightly turn when the train approaching each station. The range motions created will be around  $1.47 \text{ m/s}^2$  in deceleration. And the motions can reach up to  $1.45 \text{ m/s}^2$  in acceleration which is the highest movement to the right. As horizontal motion of the train basically are the most important analyses to detect the vibration, so roll angle will be analyses in order to see any changes on the vibration itself.



A roll-down motion was observed when the train slows down before entering the station platform which shows some deceleration in roll angle until its slightly almost  $0^\circ$  degree when the train stop. So it shows that the train in static motion which no roll angle were detected. As the train starts to move for the next station, the roll angle shows some angle either in negative and positive angles as the train probably would turns into left and right as it starts moving. So the negative angle shows the train move towards left while the positive angle move towards right motion. But as it shows in the Figure 37, the roll motion shows some spikes starting from Rawang area to Kuala Lumpur station. As z-axis acceleration shows some disturbance on the vibration in this area, it could affect other motions as well.

### 4.3.2 Track Characteristics

From the collected data from the train-mounted field testing, it shows some relationship between each featured into mapping system to differentiate and understand the motions and curvature of the track itself. When the train on the straight track, it shows almost zero curvature and could help the train to travel in higher speeds compare than the banked curvature. Vibration shows more changes frequently starting at Rawang station.

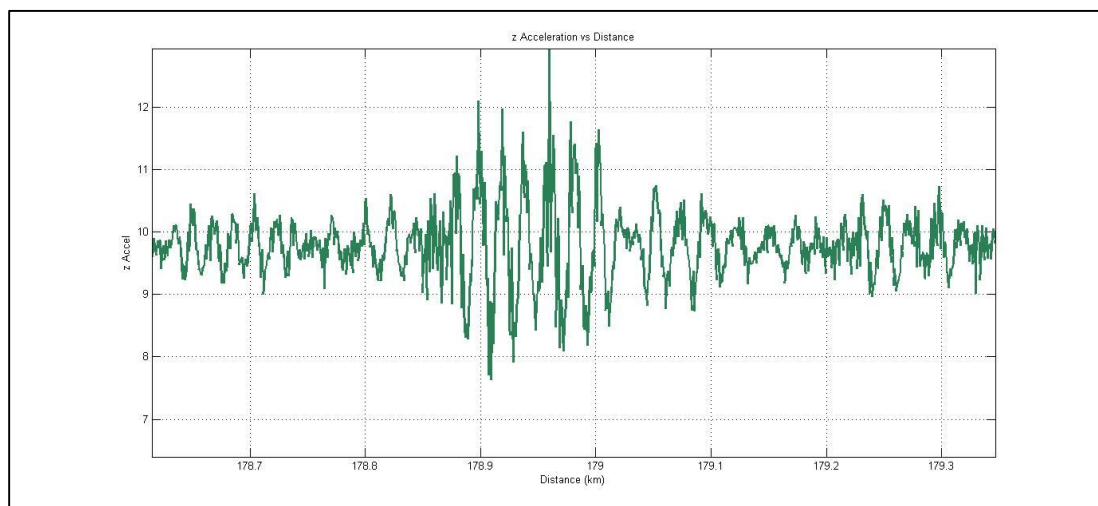


FIGURE 41. z axis acceleration measurement in KM178.6 to KM179.3.

Figure 41 above shows the highest vibration measurement data from z-axis acceleration in KM178.6 to KM179.3. Around 700 meter was observed on the track between that distance could create highest magnitude changes in vertical direction. While in Figure 42 below shows the acceleration of y-axis acceleration for the right

motion of the train. As the highest magnitude could create within KM142.5 to KM145.5. Around 3.0 kilometer of the track moved towards right motion.

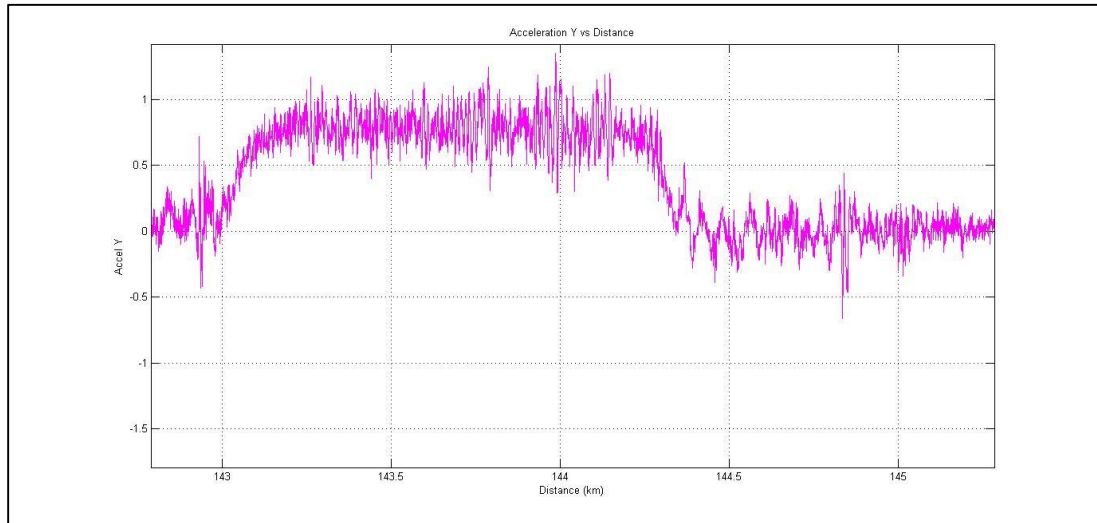


FIGURE 42. y axis acceleration between KM142.5 to KM145.5

When the highest acceleration that was observed within KM181.25 to KM186.5 as shown in Figure 43. In between 5.25 Kilometer of the track were design to move toward into left direction.

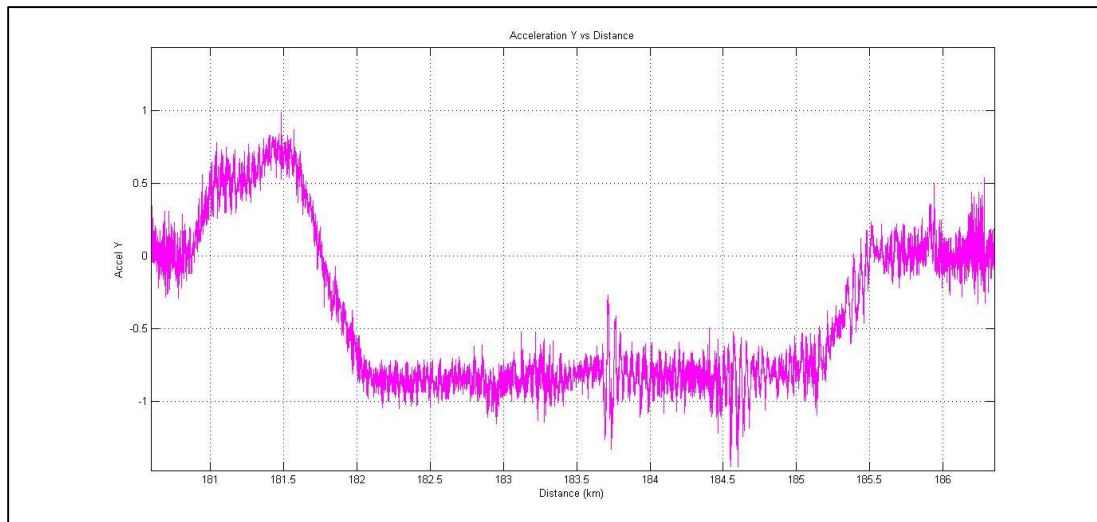


FIGURE 43. Vertical acceleration measurement in KM181.25 to KM186.5.

By using roll angle motion of the graph, a banked curvature of the train track can be identified by the data of decreasing and increasing of the roll angle itself. As the train passes through these curvature, the y-axis acceleration was observed to have an effect to overflow and saturate at a constant value. Consequently the determination of the train track at curvature needs to depend on its roll motion.

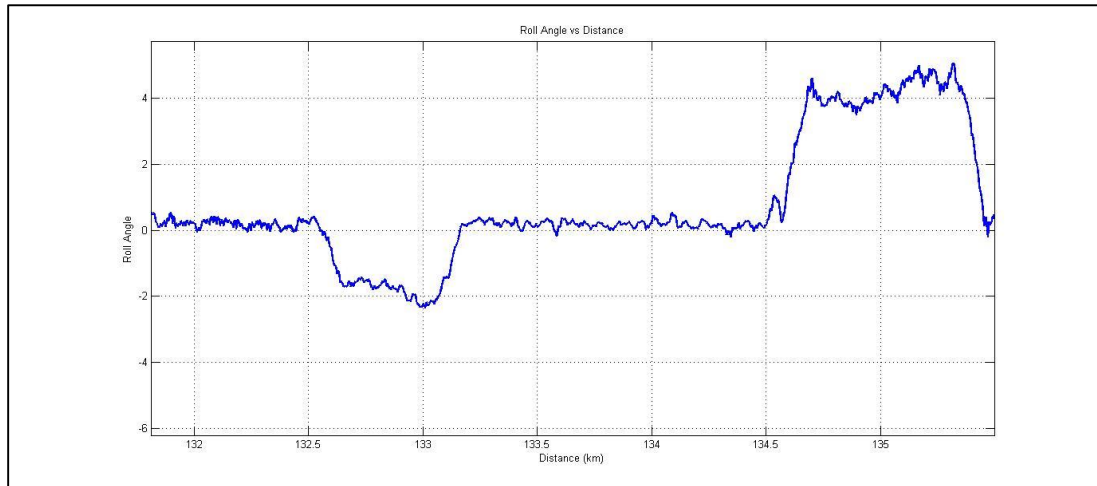


FIGURE 44. Roll angle measurement in KM132 to KM135.5

Figure 44 above shows the measurement data of roll angles as the train passes through two banked curvature. When in the graph shows that in KM132.5 to KM133.2 in maximum angle around  $-2.33^\circ$  which the train moved towards left around 70 meters, while follows the motion in smooth and slightly static on track for 1.3 kilometers before it slightly shows some curvature around 1000 meters the train roll in maximum  $5.07^\circ$  angle towards right motion in distance of KM134.5 to KM135.5.

### 4.3.3 Conclusion

As shown in Figure 37 and Figure 38, abnormalities of train track can be identified along the way from Rawang to Kuala Lumpur stations. This is probably due to the misalignment of the track, or abnormalities of nature that might affects the movement of the train. As from Rawang itself, the track was under maintenance and old due to this area is place for unused train that was left out for maintenance. Due to this, it may affect the ground and probably the vibration may affect due to the components of the train is on the track. In order to be more accurate, data collections should be done more to see the comparison of vibration movement. Even the data partially proved to show some clear abnormalities of the train's track, but further investigation could helps in term of more reasons on how the vibration could be solved. Improvement could be done by applying few IMU sensors and be mount on train couch for each side (left and right) so that the output of the data could be identify for each side of the train's coach.

## CHAPTER 5

### CONCLUSION AND RECOMMEDATIONS

#### 5.1 Conclusion

The main reason of aiming the development of train track misalignment detection system to enhance the possibility of vibration systems in any misaligned railway system, improvement in term of maintenance and thus to provide good riding experience for passengers. Plus, the vibration can be also included based on the interaction between train and the railway itself as the data collected can be acted as one of the precaution for any misalignment of the track.

IMU, which consists of gyroscope and accelerometer, will be used in order to get the reading on the train motion and orientation. The data collected from the IMU will be transferred into a PC system for data collection and data post-processing.

DCM algorithm is required to compensate drifting error from gyro sensors based on reference data from the accelerometer. At the end of this project, expected system must be in a portable design, can be widely used in train system, and simple installation.

#### 5.2 Recommendation

The GPS mapping technique could be useful in order to display the actual location of the train, thus it helps to improve the feasibility and accuracy of the system. While it helps to get the locations for any tracks that shows more vibration changes, so that prevention can be made before any consequences happens.

Different type of IMU give different type of output follows their own criteria and datasheet. By choosing specific IMU that have ability to detect the misalignment can be improve by using different type of IMU sensors. This is due IMU sensors got new interfaces in order to be competitive and feasible in worldwide usage.

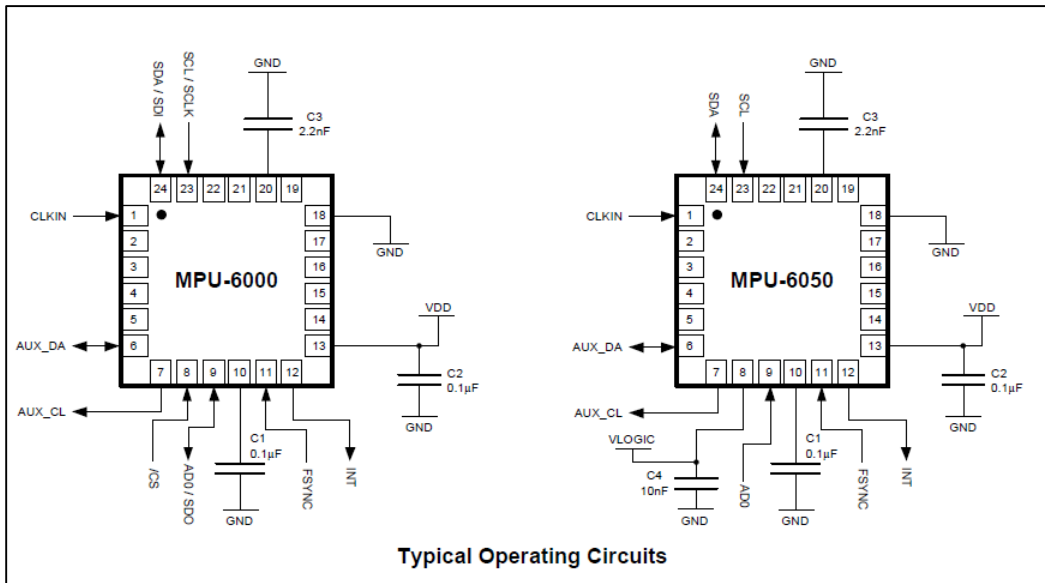
Another improvement can be made to obtain good system which is the placement of the sensors on the compartments, well-designed controlled algorithm and accurate sensor calibration.

## REFERENCES

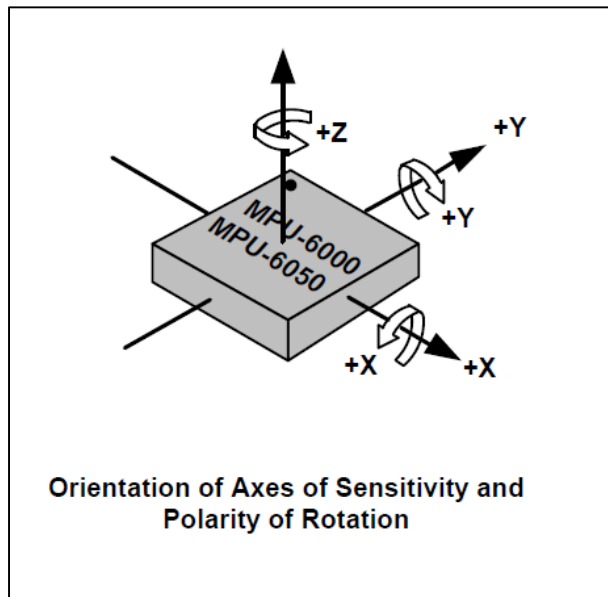
- [1] D. M. Lowtan, "Rail System in Malaysia," *Massachusetts Inst. Technol.*, pp. 1–16, 2004.
- [2] "Train Facts - Interesting Facts about Trains and Railroads." [Online]. Available: <http://www.trainhistory.net/train-facts/>. [Accessed: 17-Oct-2015].
- [3] B. Ellya and M. Ahmad, "Malaysia : Key Logistics and Transport System ( Road and Rail )."
- [4] the free encyclopedia Wikipedia, "Rail transport in Malaysia." [Online]. Available: [https://en.wikipedia.org/wiki/Rail\\_transport\\_in\\_Malaysia](https://en.wikipedia.org/wiki/Rail_transport_in_Malaysia). [Accessed: 16-Dec-2015].
- [5] K. S. Manusia, "OCCUPATIONAL ANALYSIS AUTOMOTIVE INDUSTRY Department of Skills Development." Department of Skills Development Ministry of Human Resources Level 7-8, Block D4, Complex D Federal Government Administrative Centre 62530 Putrajaya, Malaysia, p. 391, 2012.
- [6] T. S. LEE, "AN ANALYSIS OF THE DEMAND FOR PASSENGER RAIL SERVICES IN PENINSULAR MALAYSIA," 2002.
- [7] A. Roza, S. Koting, and M. R. Karim, "Intercity Land Public Transport Challenges in Developing Country : A Case Study in Peninsular Malaysia," *Proc. East. Asia Soc. Transp. Stud.*, vol. 9, pp. 1–20, 2013.
- [8] N. S. Abdul Sukor, M. Subramaniam, and M. I. Mohd Masirin, "Punctuality of Intercity Trains and Passengers ' Perspective towards Arrival Time Delay," *Res. J. Appl. Sci. Eng. Technol.*, vol. 5, no. 6, pp. 1998–2002, 2013.
- [9] S. Schwarcz, "Public Transportation In Kuala Lumpur, Malaysia," p. 24, 2003.
- [10] S. L. Ho, "Futuristic railway condition monitoring system," *Railway Engineering - Challenges for Railway Transportation in Information Age, 2008. ICRE 2008. International Conference on*. pp. 1–9, 2008.
- [11] S. Samal, A. Bhattaacharyya, and S. K. Mitra, "Study on Corrosion Behavior of Pearlitic Rail Steel," vol. 10, no. 7, pp. 573–581, 2011.
- [12] S. Kaewunruen and A. Remennikov, "Dynamic properties of railway track and its components: a state-of-the-art review," *New Res. Acoust.*, pp. 197–220, 2008.
- [13] J. Sadeghi and P. Barati, "Evaluation of Conventional Methods in Analysis and Design of Railway Track System," *Int. J. Civ. Eng.*, vol. 8, no. 1, pp. 44–56, 2010.
- [14] K. Goser, K. Schuhmacher, M. Hartung, K. Heesche, B. Hesse, and A. Kanstein, "Neuro-fuzzy systems for engineering applications," *AFRICON, 1996., IEEE AFRICON 4th*, vol. 2. pp. 759–764 vol.2, 1996.
- [15] D. C. S. Clair, D. Mellor, B. Flachsbar, and R. Reed, "Using Neural Networks To Automate the Detection of Rail," *Society*, vol. 4.

- [16] O. Jarrah, "Fault detection and accommodation in dynamic systems using adaptive neurofuzzy systems," *IEE Proc.-Control Theory Appl.*, vol. 148, no. 4, p. 283, 2001.
- [17] H. Li, X. Zhou, K. Yang, and L. Luo, "A wheel treads flat detection system for high-speed railway," *Electrical & Electronics Engineering (EESYM), 2012 IEEE Symposium on.* pp. 59–62, 2012.
- [18] T. Fujita and M. Idesawa, "New Types of Position Sensitive Device for Accurate Sensing Graduate School of Information Systems," *Structure*, vol. 2.
- [19] J. Suzuki, T. Murakami, and K. Ohnishi, "Position and force control of flexible manipulator with position sensitive device," *Advanced Motion Control, 2002. 7th International Workshop on.* pp. 414–419, 2002.
- [20] C. Weiming, Z. Weina, S. Wei, L. Liang, and S. Guiqing, "Straightness Measurement for Long-length Rails of Bridge Crane," *Measuring Technology and Mechatronics Automation (ICMTMA), 2011 Third International Conference on.*, vol. 3. pp. 354–357, 2011.
- [21] C. T. Incorporated and C. Technologies, "Cytron USB to UART Converter User ' s Manual," no. June, pp. 1–23, 2011.
- [22] "IntroductionPage - ardu-imu - Arduino based IMU & AHRS - Google Project Hosting." [Online]. Available: <https://code.google.com/p/ardu-imu/wiki/IntroductionPage>. [Accessed: 08-Dec-2015].
- [23] SparkFun Electronics ®, "DIYDrones ArduIMU+ V3." [Online]. Available: <https://www.sparkfun.com/products/11055>. [Accessed: 08-Dec-2015].

## APPENDIX



Appendix 1



Appendix 2